TR 607—FINAL

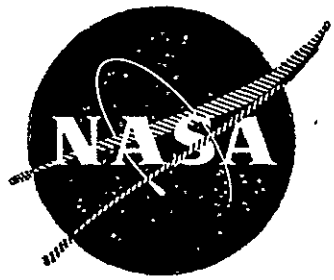

CAVITATION DAMAGE IN LIQUID METALS

Potassium Studies)

by

A. Thiruvengadam, S. L. Rudy and H. S. Preiser

prepared for

NATIONAL AERONAUTICS AND SPACE ADMINISTRATION

CONTRACT NAS 3-8506

APRIL 1968

HYDRONAUTICS, incorporated
research in hydrodynamics

rch, consulting, and advanced engineering in the fields of NAVAL and INDUSTRIAL HYDRODYNAMICS. Offices and Laboratory in the Washington, D. C., area: Pindell School Road, Howard County, Laurel, Md.

(over)

NOTICE

This report was prepared as an account of Government sponsored work. Neither the United States, nor the National Aeronautics and Space Administration (NASA), nor any person acting on behalf of NASA:

(a) Makes any warranty or representation, expressed or implied, with respect to the accuracy, completeness, or usefulness of the information contained in this report, or that the use of any information, apparatus, method, or process disclosed in this report may not infringe privately owned rights; or

(b) Assumes any liabilities with respect to the use of, or for damages resulting from the use of any information, apparatus, method or process disclosed in this report.

As used above, "person acting on behalf of NASA" includes any employee or contractor of NASA, or employee of such contractor, to the extent that such employee or contractor of NASA, or employee of such contractor prepares, disseminates, or provides access to, any information pursuant to his employment or contract with NASA, or his employment with such contractor.

Requests for copies of this report should be referred to:

National Aeronautics and Space Administration
Office of Scientific and Technical Information
P. O. Box 33
College Park, Maryland 20740

HYDRONAUTICS, Incorporated

T. R. 607-FINAL

CAVITATION DAMAGE IN LIQUID METALS (POTASSIUM STUDIES)

By

A. Thiruvengadam, S. L. Rudy
and
H. S. Preiser

Prepared for

National Aeronautics and Space Administration
April 1968
Contract No. NAS 3-8506

Technical Management
NASA Lewis Research Center
Cleveland, Ohio
Space Power Systems Division
James P. Couch

HYDRONAUTICS, Incorporated
Pindell School Road
Laurel, Maryland

FOREWORD

The work described herein was performed by HYDRONAUTICS, Incorporated, Laurel, Maryland, under NASA Contract NAS 3-8506, to study the resistance of candidate materials to cavitation damage in high temperature liquid potassium. Mr. James P. Couch of the Space Power Systems Division, NASA - Lewis Research Center, was the technical manager.

ABSTRACT

This is the final report of studies on the relative cavitation damage resistance in high purity liquid potassium of five candidate materials for use in high output, Rankine-cycle space power systems. Results of tests on TZC, Cb-132M, TiC + 10% Cb binder, 316 stainless steel and T-111 are presented. The effects on damage resistance of liquid potassium temperature (up to about 1200°F) and argon pressure above the liquid potassium surface, are described. Of the metals tested TiC + 10% Cb is found to exhibit the best erosion resistance up to about 900°F. The rate of erosion is significantly dependent on both the temperature and the argon pressure. It may be stated that in general, the rate of damage increases with temperature and then decreases, and also that the rate of damage is small at sub-atmospheric pressures.

TABLE OF CONTENTS

LIST OF FIGURES

SUMMARY

This is the final report of studies on the relative resistance of TZC, Cb-132M, TiC + 10% Cb binder, 316 stainless steel and T-111 to cavitation erosion in high purity liquid potassium. Both TZC and Cb-132M were tested in two heat treatments, namely, stress relieved and recrystallized. Each showed good erosion resistance, the stress relieved state performing better than the recrystallized form for both metals. The rate of erosion for TZC and Cb-132M attained peak values at 600°F and 800°F respectively, falling off considerably at both lower and higher temperatures. Of the metals tested, Ti-C + 10% Cb exhibited the best cavitation resistance in the steady state at 600°F, but the poorest resistance at temperatures higher than about 900°F. Around 1200°F, 316 stainless steel showed the best resistance. Further, the erosion rate of TZC and 316 stainless steel generally increased as the argon pressure in the retort was increased from zero to 40 psia at constant temperature. An anomalous behavioral pattern was found in the tests conducted on T-111 at elevated temperatures and this behavior was believed to be attributable to the high sensitivity of T-111 to oxygen. The details of this experiment are contained in the Appendix.

INTRODUCTION

High output Rankine-cycle space power systems will utilize nuclear reactors as their principal sources of energy. These systems will require the use of alkali metals as heat transfer and working fluids operating at temperatures up to 2200°F. Such power systems will be required to provide reliable performance for 1 to 3 years of unattended service. However, because the liquid condensate in these systems will be transferred under transient conditions conducive to the formation of vapor bubbles, problems due to cavitation can be envisaged. A reduction of the cavitation in the systems can be achieved by sub-cooling the liquid but this would culminate in increasing radiator requirements and incurring serious penalties in the system weight. The best compromise appears to be to allow the pump and other low pressure points in the condensate system to operate with some degree of cavitation and to use materials which are most resistant to cavitation to withstand the damage. It is the objective of this program to determine what materials are most resistant to cavitation and also the conditions under which their resistance can be enhanced.

HYDRONAUTICS, Incorporated, has been engaged in cavitation damage research for the past several years using a magnetostriction device to vibrate metal specimens in various liquid media. The NASA supported research has included tests in water and high temperature (up to 1500°F) liquid sodium. The latter work was conducted in an experimental facility which incorporated a magnetostriction transducer into a vacuum chamber with additional

provisions for an integral, liquid metals transfer, storage and purifying circuit. Utilizing a modified version of this facility, the present program extends the tests to include those in high temperature liquid potassium. The cavitation damage encountered by 316 stainless steel, TZC, T-111, Cb-132M, TiC + 10% Cb, was determined over a wide temperature range up to 1300°F.

Previous tests have shown that the damage rate decreases rapidly with increasing temperature at a constant ambient pressure level. This is explainable by the fact that since vapor pressure increases with temperature, the driving pressure, namely the ambient pressure minus the vapor pressure, which is related to the collapsing forces on the cavitation bubbles of the previous tests was decreasing with increasing temperature. In addition to determining the relative cavitation damage resistance of the aforementioned materials in liquid potassium at constant temperature and ambient pressure, some tests were conducted on 316 stainless steel and TZC alloy to show the influence of ambient pressure on cavitation damage resistance.

APPARATUS

The experimental facility consists essentially of the following systems: (Figure 1)

1. Controlled Environment Dry Box
2. Cover Gas Systems
3. Liquid Metal System
4. Heating and Cooling Systems
5. Magnetostriction Apparatus

Controlled Environment Dry Box

This is a 304 stainless steel chamber designed to be evacuated to a minimum pressure of 3 millitorr prior to back-flushing with pure argon cover gas. A standard sloped-front dry box was modified with special access openings for an air lock, heated specimen lock tubular housing for the magnetostriction device, rear door view ports, lighting ports, utilities and instrument connections. A false bottom is fabricated in the box for cooling purposes. The general arrangement is shown in Figure 1.

The pressure in the dry-box was measured at 4 millitorr. Rise of pressure with time inside the dry-box was recorded over several runs and was found to average about 35 millitorr per hour.

Cover Gas System

An inert atmosphere of pure argon surrounds all components which are in contact with or have access to the liquid alkali metal. Commercially available, high purity argon, with total

moisture, oxygen and nitrogen of less than 5 ppm, is used to fill the dry box, retort, air lock and specimen lock after evacuation. The argon gas was monitored at the manifold prior to entering the dry box and was found to contain 0.5 ppm O_2 and 1.5 ppm H_2O. With the glove port covers in place, the moisture rose almost linearly from 1.5 to 5 ppm in one hour and the oxygen climbed rapidly to about 3.5 ppm and then remained practically constant for the one hour run. Figure 2 shows the moisture and O_2 rise as a function of time. The rise in moisture and oxygen with the glove ports open was also recorded. Figure 3 shows the rate of rise of moisture and O_2. Average rate of rise for oxygen is about 12 ppm/hr and for moisture, 30 ppm/hour.

Liquid Metal, Heating and Cooling Systems

Retort System

A retort for liquid alkali metal service capable of withstanding 1300°F and pressures from 10^{-3} torr to 50 psig was constructed of a 5-inch diameter 304 stainless steel tube having a wall thickness of 1/4 inch. A suitable end cap was welded on the bottom end of the tube to which was fitted the fill and drain piping system. The upper end of the retort was fitted with a mating flange which bolted directly to the floor of the dry box, and was sealed with a metal O-ring. A screen was placed over the drain hole to prevent large particles of foreign material from entering the liquid alkali metal piping system. The entire fabrication of this component conformed to highest commercial standards for nuclear service. All welds were helium leak tested

and found to be free of defects. The essential details of the retort system are shown in Figure 4.

The head of the retort incorporates a vapor trap system which vents into the dry box. A pressure gage was fitted into the vent system for measuring retort pressures. The schematic details of the vapor trap system are also shown in Figure 4. This arrangement will permit the retort pressure to be maintained at any level independent of the dry box pressure. Whenever specimens are to be removed from the retort for observation and weighing, the retort pressure is equalized to box pressure by either venting the retort atmosphere into the dry box at higher retort pressures or by venting the dry box atmosphere into the retort at lower retort pressures. The vapor trap is cooled by fastening the entire assembly to the water-cooled floor of the dry box.

One of the thermocouple wells (short) in the retort head was a heavy Inconel-sheathed, grounded thermocouple inserted through a suitable fitting to make direct contact with the upper level of potassium in the retort. This arrangement permits fast thermal response and allows the thermocouple to be used as a secondary liquid level indicator. The primary liquid level indicating method employs an electrical contact through an ungrounded probe.

Liquid Alkali Metal Transfer System

A potassium transfer system was installed, using 3/8 inch O.D. annealed 316 stainless tube (.049 inch wall). Transfer system heating was accomplished by wrapping the lines with various lengths of high-temperature fiberglass-insulated heating tape.

Each set of heating tapes can be controlled independently by an auto-transformer allowing separate heating of retort, fill and dump, or hot-trap charge lines. These glass-insulated tapes performed so efficiently that no outer thermal insulation over the piping was necessary. Thermocouples fastened to the piping by means of hose clamps are positioned at strategic locations in the piping system to permit a temperature check to be made at elbows, fittings and valves prior to the transfer of the liquid alkali metal. No trouble was experienced in transferring the liquid alkali metal to any part of the liquid metals loop. The schematic diagram of the liquid alkali metal loop is shown in Figure 5.

Hot Trap

The hot trap was cleaned and modified by replacing the existing spring-operated bellows-sealed valves (which become inoperative after long-term exposure to high temperatures) with positive-opening bellows-sealed valves.

One of the existing thermocouple wells (short) was removed and replaced by a 3/4-inch O.D., 316 stainless steel tube, .060-inch wall thickness. This larger tube, which connects to the cover gas and vacuum piping, permitted the installation of a rod-out system to clear the line of liquid alkali metal residues which were expected to accumulate during prolonged operation. A suitable vapor trap was incorporated in the cover gas and vacuum piping to confine the liquid alkali metal vapor to that section of piping containing the rod-out mechanism.

Heavy Inconel-sheathed, Chromel-Alumel, grounded thermocouples were inserted into the piping connections in the hot trap to make direct contact with the liquid alkali metal. These fast-response thermocouples provide a liquid level indicating system; a long thermocouple indicates the beginning of fill and the short thermocouple indicates the upper level of filling for the hot trap. This system has worked so well that the design of a direct weighing system for measuring the amount of liquid alkali metal charge in the hot trap was abandoned.

The hot trap is cycled automatically to maintain a 1250°F temperature overnight for 12 hours and then cooled down so that the liquid alkali metal can be transferred at about 500°F at the start of the working day. A high-temperature safety cutout on the hot trap furnace prevents the possibility of over-heating during unattended periods. Figure 6 shows a schematic diagram of the modified hot trap and associated instrumentation.

Magnetostriction Apparatus

The magnetostriction apparatus (Figure 7) vibrates a test specimen rapidly in the hot liquid alkali metal to form cavitation bubbles during the upstroke which collapse on the specimen during the downstroke, to produce the desired damage. This repetitive cycle leads to measurable damage rates under carefully controlled laboratory conditions.

The magnetostriction apparatus consists of a nickel transducer and velocity transformer, which is caused to oscillate in a resonant condition by an alternating magnetic field furnished from a sine generating power supply as shown in Figure 7. The apparatus was housed in a suitable elevating mechanism to permit operation in the dry box. A simple strain gage cemented to the stack has provided an adequate monitoring signal for determining amplitude of vibration of the specimen.

A feed-back control circuit was also incorporated in system electronics which provided continuous stable frequency and amplitude output of the apparatus despite local fluctuations in operating temperature gradients. The details of design have been described in Reference 1.

The transducer stack was air-cooled. When the air-cooling system was operated, the air outlet temperature, at 0.5 cfm directed at the stack, was recorded to be $54^{\circ}F$. Under these conditions, the stack temperatures at full power remained below $150^{\circ}F$ which is considered to be satisfactory.

EXPERIMENTAL PROCEDURE

Cavitation Damage Resistance Tests

Reference 2 presents a detailed study of the effect of various test parameters on the cavitation damage produced by a magnetostriction device. The reproducibility of results with a simple flat faced test specimen is equivalent to other more complex specimen shapes. The dimensions of the liquid container within wide limits have a relatively insignificant effect on the test results. The same conclusion holds good for the depth of immersion of the specimen in the test liquid. The rate of volume loss varies as the square of specimen diameter in the steady state zone.

Based on these observations, the following test parameters used in this program were selected: A simple flat faced specimen of half an inch radius was vibrated at a double amplitude of 1.40×10^{-3} inch and a frequency of 14 kcs to obtain the relationship between the damage rate and the test duration until the steady state zone was reached.

Until recently it has been the general practice to test all materials over an arbitrarily selected constant duration, and to compare the cumulative damage as an indication of the cavitation damage resistance. However, it is now known that the rate of damage is time dependent (References 2, 3, 4) and this relationship can be divided into four different zones of damage:

(a) Incubation zone - The incubation zone has been defined as the time during which "little" or no weight loss occurs.

(b) Accumulation zone - After incubation, the material starts absorbing more and more energy giving rise to increased fracture and weight loss.

(c) Attenuation zone - The rate of damage reaches a peak in the accumulation zone and then begins to decline. The beginning of this zone is characterized by isolated deep craters.

(d) Steady state zone - The zone in which the rate of weight loss reaches a constant value after declining in the attenuation zone. In this zone the cavitation damage rate is observed to be time independent and thus far it is in this zone that the most successful correlations of cavitation damage with material parameters have been made. The existence of these zones have been confirmed for several metals and in various liquid environments (Reference 4).

To make a meaningful comparison of the performance of the five metals tested under this program, the relationship between the test duration and the rate of damage were obtained and are shown in Figures 8 through 15 at 600°F. Each data point represents one measurement of volume loss.

The fact that the curves in Figure 15 cross each other indicates that each one of the five metals tested exhibits its own characteristic response. An explanation of these specific response characteristics in the first two zones is considered possible through better understanding of the behavior of these metals

at high rates of straining at elevated temperatures and of the process of energy accumulation during repeated loading. An understanding of the third zone of damage, the attenuation zone (characterized by the formation of isolated deep craters) is related to the surface roughness of the material which in turn affects the hydrodynamics of bubble collapse (Reference 2). This view is supported by some recent experimental evidence indicating that artificial roughness simulating cavitation damage will eliminate or reduce the peak in the transition to the steady state zone (Reference 4). More detailed investigations are required to resolve these aspects of the damage rate behavior.

It should be noted that the experiments beyond 600°F were conducted with the same specimens that were used to obtain the steady state zone at 600°F liquid alkali metal. This procedure was adopted because the relatively lower rates of damage observed at higher temperature would require inordinately long testing periods to achieve damage in the steady zone. Some initial experiments reported in Reference 5 showed that only surface indentations could be observed on 316 stainless steel at 1000°F even after 25 hours of testing. However, the use of specimens prepared in the steady state zone at another temperature was considered valid in view of the fact that previous data had shown that specimens prepared in the steady zone at one intensity (amplitude) continued to damage at a constant but different rate at another amplitude.

Oxide Impurity Level in Liquid Alkali Metal

Calibrations were made to determine the oxide impurity level of liquid alkali metal heated in the retort and exposed to the dry box atmosphere over a normal 8 hour working period. The potassium had to be transferred from the storage drum to the hot trap where it was hot-trapped for a minimum of 72 hours at 1250°F. Liquid alkali metal sample capsules were made from 3/4 inch diameter, 0.028 inch wall, 316 stainless steel tubing, 6 inches in length and capped on both ends. The capsules were degreased in acetone, carefully washed and baked out in vacuum prior to use. Each capsule contained a 20-gram sample of the liquid alkali metal. Each of the samples was taken by the dip tube method. Several dips were required to fill a sample capsule with the liquid alkali metal. During the first sampling period, representing about 4-1/2 hours of a normal working day, glove ports were operated intermittently, the elevating mechanism was operated and a specimen was tested and removed from the box through the specimen lock. The dry box was pumped down after the first sampling when the moisture level rose to 65 ppm. The samples were sent to Atomic Power Development Associates in Detroit, Michigan for analysis by a modified mercury amalgamation technique. The results are shown in Table 1. Samples were taken periodically throughout the program and these results are also shown in Table 1.

EXPERIMENTAL RESULTS AND DISCUSSION

A. Relative Erosion Resistance of Refractory Alloys

(1) Materials Tested Under this Program: The following materials were tested under this program.

a. 316 stainless steel
b. T-111
c. Cb-132M
d. TZC
e. TiC + 10% Cb binder

The materials Cb-132M and TZC were tested in two heat treated forms, namely, stress relieved and recrystallized. The metallurgical compositions and the conditions of heat treatment are summarized in Table 2. The surfaces of the eroded specimens after all the tests were completed are shown in Figure 16.

(2) Results of Erosion Tests on these Materials: Figures 8 through 14 show the rate of volume of material eroded as a function of test duration for all the materials tested under identical test conditions in liquid potassium. Figure 15 shows a summary of these test results. A comparison of the cavitation damage r sistance of all the materials tested can be made easily from Figure 15.

B. Effect of Potassium Temperature on the Rate of Erosion

The second major objective was to determine the effect of potassium temperature on the rate of erosion of the materials cited above. Figures 17 through 21 show how the rate of volume

loss depends upon the liquid temperature. A summary of these data is shown in Figure 22 for the sake of comparison. The general trend is that the rate of volume loss increases with temperature and then decreases. A discussion of these results in the light of the knowledge available at present is presented later in this report.

C. Effect of Pressure on the Rate of Erosion

The relationship between the potassium pressure and the rate of erosion for 316 stainless steel and TZC (stress relieved) at three different temperatures, namely 600, 900 and 1200°F is shown in Figures 23 through 28. A summary of all these results is given in Figure 29.

D. Analysis of Results

(1) Effect of Test Duration: The present experimental results essentially confirm the earlier findings (References 1,5) that the rate of erosion increases with testing time, reaches a peak, then decreases and becomes independent of test duration. Figures 30 and 31 show this relationship both in liquid sodium and liquid potassium at the same temperature (400°F) for the same material (316 stainless steel). All of our investigations on the relative erosion resistance of metals, and on the effects of liquid temperature and pressure were conducted in the time-independent region called the steady state zone (See Experimental Procedure). In this zone the cavitation damage resistance of a material is best characterized by its fracture strain energy. Where, all other factors being equal, the greater the strain energy the greater the resistance of the material to cavitation damage.

(2) Relative Erosion Resistance of Refractory Alloys: As shown in Figure 15, the materials tested in potassium may be placed in the following relative order of cavitation damage resistance starting from the best as compared in the steady state at 600°F:

a. TiC + 10% Cb
b. TZC (stress relieved)
c. Cb-132M (stress relieved)
d. Cb-132M (recrystallized)
e. TZC (recrystallized)
f. T-111
g. 316 stainless steel

The recrystallized form of Cb-132M and TZC exhibit lower erosion resistance as compared to the stress relieved condition in both cases. This seems reasonable from the point of view of the strain energy criterion since stress relieving improves the ductility of the metals thereby improving the elongation.

The observed differences in erosion rates between the recrystallized and stress relieved forms of Cb-132M and TZC are believed to be significant since the shape of the curves in the earlier zones of damage (accumulation and attenuation) are markedly different. The area under the damage curves is representative of the energy absorbed by the metals to produce sustained fracturing. Further detailed treatment of these earlier zones of damage are found in Reference 1.

The trend of the relative erosion resistance of the various materials tested remains essentially the same in the entire temperature range with the exception of 316 stainless steel which shows superior resistance around 1200°F (see Figure 22).

(3) Effect of Potassium Temperature on the Intensity of Cavitation Erosion: One of the important parameters controlling the intensity of cavitation erosion is the temperature of the cavitating liquid. It has been known for a long time that the rate of erosion increases with temperature, reaches a peak and then decreases with increasing temperature. A summary of the results obtained by various investigators using a magnetostriction device is given in Reference 6. Similar results for liquid sodium are given in Reference 1. In all of the above investigations, the relationship between the rate of erosion and the temperature was solely explained in terms of the physical properties of the liquid. (See for example References 7, 8 and 9). At lower temperatures the damage increases with increasing temperature because the solubility of the non-condensible gases (argon in the case of potassium) decreases with temperature. Whereas at higher temperatures, the vapor of the liquid acts as a damper cushioning the bubble collapse pressures. These explanations are quantitatively demonstrated in Reference 9 for liquids such as water, benzene, aniline and toluene.

However, the present investigations show (Figure 15) that the material plays an important role since the temperature at which the rate of erosion is maximum is about 600°F for materials

like TZC and 316 stainless steel whereas the peak occurs around 800°F for T-111 and Cb-132M. The erratic behavior of the T-111 specimen at 1200°F was not understood despite some careful repetitions of the experiments which are described in the Appendix. However, T-111 is known to be very sensitive to oxygen at elevate temperatures.

The material TiC + 10% Cb binder exhibits a peculiar characteristic in that the minimum rate of erosion occurs around 600°F and the maximum rate in the range of 1000° - 1200°F. Titanium carbide is known to exhibit intergranular attack under impingement exposure in high temperature lithium (Reference 10). This mechanism may also explain marked changes in erosion damage observed in the high temperature region of these potassium experiments.

A literature survey was made to collect the available mechanical properties data for the four test metals at different temperatures and these data are presented in Figures 32 through 35. The estimated strain energy from these data are shown in Figure 36 as a function of temperature. While the strain energy of two metals that exhibit the peak rate at 600°F namely TZC and 316 stainless steel decrease monotonically with increasing temperature, the strain energy of the other two metals (Cb-132M and T-111) reach a minimum value at 800°F and this temperature coincides with the temperature corresponding to the peak rate of erosion.

(4) Effect of Pressure on the Rate of Erosion: Peters and Rightmire (Reference 6) conducted experiments as early as 1938 on the effect of pressure on cavitation erosion. The results of their experiments with water at 100°C using brass specimens, are shown in Figure 37. Later on Leith and Thompson (Reference 11) also investigated the effect of ambient pressure on the cavitation erosion of materials and their results are shown in Figure 38. The results of these authors show that the rate of erosion increases with increasing pressures and reaches a peak around atmospheric pressure of 15 psia. At values above atmospheric pressures, Peters and Rightmire observe a pronounced second peak whereas the results of Leith and Thompson do not show such a second peak. The results of the present experiments (shown in Figure 29) confirm the results of both references. At 600°F the rate of erosion is a maximum around 20 psia, reaching a minimum at 30 psia and then increasing up to 40 psia. This trend is true both for 316 stainless steel and TZC and is similar to the results of Peters and Rightmire shown in Figure 37. At higher temperatures, the results are similar to those of Leith and Thompson (Reference 11), shown in Figure 38. An explanation of these results may be sought by analyzing the dynamics of bubble collapse and how the pressurization of the liquid affects the bubble collapse. One fact is that the dissolved gas content in potassium, from the gas used for pressurization, would very much depend upon both the pressure and temperature. In addition, the violence of the collapse pressure also depends upon the surrounding pressure.

According to a recent analysis (Reference 9) based on the work of Rayleigh (Reference 12) and Noltingk and Neppiras (Reference 13), the collapse pressure is given by

$$P_c\Big|_{\text{isothermal}} = \frac{P_o}{6.35} \exp\left(P_o/Q_o\right)$$

and

$$P_c\Big|_{\text{adiabatic}} = \frac{P_o}{6.35}\left(\frac{P_o}{4Q_o}\right)^3$$

where

$P_c\Big|_{\text{isothermal}}$ is the collapse pressure when the bubble collapse is isothermal,

$P_c\Big|_{\text{adiabatic}}$ is the collapse pressure when the bubble collapse is adiabatic,

P_o is the characteristic pressure field acting on the bubble, and

Q_o is the partial pressure of non-condensible gases dissolved in the liquid.

An explanation of why peak rates occur around certain temperatures and pressures can only be possible through a more detailed analysis of the dynamics of the bubble collapse. However, the significant result is that the rate of erosion can be reduced by reducing the pressure.

CONCLUSIONS

An analysis of the test results pertaining to the cavitation damage resistance of TiC + 10% Cb, TZC, Cb-132M, 316 stainless steel and T-111 leads to the following conclusions:

1. Of the metals tested TiC + 10% Cb exhibits the best erosion resistance in liquid potassium up to about 900°F.

2. The stress relieved form of TZC and Cb-132M gives better erosion resistance as compared to their performance in the recrystallized condition.

3. The rate of erosion depends significantly on the temperature of the liquid potassium. In general the rate of damage increases with temperature and then decreases. However, the energy absorption characteristics of the test material seems to have substantial influence on the above relationship.

4. The argon pressure above the liquid potassium surface seems to have a great influence on the rate of erosion. A general conclusion is that the rate of damage is small at subatmospheric pressures.

APPENDIX

T-111 Experiment

The rate of volume loss with increasing testing time for T-111 in the stress relieved condition*, was obtained at a potassium temperature of 600°F. Steady state condition was achieved in 7 to 8 hours: (see Figure 13). A regular, silvery, matte finish, was observed on the eroded surface of the T-111 specimens, very similar to that obtained on 316 stainless steel.

These steady state specimens were then run at the preselected liquid potassium temperatures to determine the effect of liquid temperature on the rate of volume loss for T-111. A peak rate of damage occurred at 800°F. Figure 19 shows the rate of damage as a function of temperature. Of major interest is the behavior of the damage rate for T-111 above 1000°F. When the same T-111 specimens, previously tested at temperatures from 400 to 1000°F, were tested in 1200°F liquid potassium, the observed rate of volume loss was consistently 5 times the rate noted at 1000°F.

The potassium in which the 1200°F tests were conducted was the same batch that had been used for the previous T-111 temperature series. However, the 1000°F and 1200°F tests were run on two consecutive days. Sometime during the night of this test period there was a brief power interruption which stopped the vacuum pump. (It is standard practice to continue evacuation of the dry box

---

* Heat treatment: Stress relieved 1 hour at 2000°F, (V.C.)

chamber during the night after testing is completed). Due to the particular electrical connections, (for safety) the vacuum pump does not normally restart when the power is restored unless the relay is manually tripped. The stopping of the vacuum pump allowed the box to back fill slowly with air (through the vacuum pump) and by morning the dry box chamber was found to be at atmospheric pressure. Even though the box chamber was filled with air, the retort was still sealed from the chamber and vacuum system which is normal practice. Standard clean up conditions were begun by evacuation of the chamber for 2 hours, back filling, with pure argon, and leaving it for 20 minutes at atmospheric pressure. After this, the box was again evacuated to a pressure of 10 millitorr and then once more back filled with fresh argon. A routine oxygen and moisture check showed that the levels were well below 15 ppm in the dry box chamber.

The potassium that was in the retort was heated to 600°F. A sample was withdrawn from the retort, and no discoloration or foreign material was observed. With this observation of the liquid metal and the fact that the retort was sealed it was decided that the potassium was not contaminated and could be used for the remaining tests. When the rate of damage of T-111 at 1200°F was unusually high as compared to previously obtained rates, a recheck test series was run. The steady state specimens were retested at 600°F to determine whether they would exhibit the same steady state rate of volume loss obtained previously. This recheck test series yielded consistent rates of volume loss which were only 1/3 of those observed before. It is known that T-111 is very sensitive to oxygen at elevated temperatures.

The cause for this reduced damage is not known. The potassium was sampled in the standard manner and dumped. The potassium sample was analyzed for oxygen contamination and found to contain 26 ppm of oxide impurity. A new batch of pure potassium was transferred to the retort, which was heated to 1000°F for one hour, then cooled to 600°F and dumped. This procedure is standard to assure complete absorption of oxides in the clean liquid metal which may have been left from a previously suspected contaminated batch of potassium. Having completed the retort cleaning, a new batch of high purity potassium was transferred to the retort and heated to 600°F. Using this potassium, a new stress relieved T-111 specimen (No. 16) was tested until it reached steady state. The rate of volume loss with time correlated well with the previous T-111 specimens as shown on Figure 13. The rate of volume loss at 1000°F for this new specimen was nearly the same as for the other specimens.

Since these data were fairly representative of previously obtained values we proceeded with the 1200°F tests. At 1200°F, the first test point, of 15 minute duration, showed a rate of volume loss of only 1/3 the rate obtained at 1000°F, and an order of magnitude less than that obtained with the previous specimens (Nos. 14 and 15). (Figure 19). A second 15 minute test showed that the rate of volume loss had increased to approximately the same as that exhibited by the two previous T-111 specimens. All other successive tests yielded the same high results. Reasons for these results are not clear.

REFERENCE

1. Preiser, H. S., Thiruvengadam, A., and Couchman, III, C.C., "Cavitation Damage in Liquid Sodium," HYDRONAUTICS, Incorporated NASA CR-54072, April 1964.

2. Thiruvengadam, A., and Preiser, H. S., "On Testing Materials for Cavitation Damage Resistance," Journal Ship Research, Vol. 8, No. 3, December 1964.

3. Thiruvengadam, A., "A Comparative Evaluation of Cavitation Damage Test Devices," Symp. Cavitation Research Facilities and Techniques, ASME, New York, May 1964.

4. Eisenberg, P., Preiser, H. S., and Thiruvengadam, A., "On the Mechanisms of Cavitation Damage and Methods of Protection, Society of Naval Arch. and Marine Engrs., Winter Annual Meeting, New York, November 1965.

5. Thiruvengadam, A., and Preiser, H. S., "Cavitation Damage in Liquid Metals," HYDRONAUTICS, Incorporated, NASA CR-72035, November 1965.

6. Peters, H., and Rightmire, B. G., "Cavitation Study by the Vibratory Method," Proceedings of the Fifth International Congress for Applied Mechanics, Topic 614-616, 1938.

7. Bebchuck, A. A., "On the Problem of Cavitation Damage to Solid Bodies," Jour. Acoustics, 3, 1, 90-91, 1957 (Soviet Physics Acoustics p. 95).

8. Plesset, M. S., and Devine, R. E., "Temperature Effects in Cavitation Damage," Report No. 85-27, Division of Engr. and Appl. Sci., California Institute of Tech., April 1964.

9. Thiruvengadam, A., "On Modeling Cavitation Damage," HYDRONAUTICS, Incorporated Technical Report 233-10, August 1966.

10. Hays, L. G., and O'Connor, D., "A 2000°F Lithium Erosion and Component Performance Experiment," JPL Technical Report 32-1150, October 1967.

11. Leith, W. C., and Thompson, A. L., "Some Corrosion Effects in Accelerated Cavitation Damage," Transactions of the ASME Journal of Basic Engineering, December 1960.

12. Rayleigh, Lord, "On the Pressure Developed in a Liquid During the Collapse of a Spherical Cavity," Phil. Mag. (6), 34, pp. 94-98, 1917.

13. Noltingk, B. E., and Neppiras, E. A., "Cavitation Produced by Ultrasonics," Proc. Phy. Soc. (London) B. 63, p. 683.

14. Metals Handbook, 1954 Supplement, The American Society of Metals.

15. The Engineering Properties of Columbium and Columbium Alloys, DMIC Report 188, Defense Metals Information Center, Battelle Memorial Institute, Columbus 1, Ohio, September 1963.

16. The Engineering Properties of Tantalum and Tantalum Alloys, DMIC Report 189, Defense Metals Information Center, Battelle Memorial Institute, Columbus 1, Ohio, September 1963.

17. The Engineering Properties of Molybdenum and Molybdenum Alloys, DMIC Report 190, Defense Metals Information Center, Battelle Memorial Institute, Columbus 1, Ohio, Sept. 1963.

18. T-111 Tantalum Base Alloy Refractory Metal, Special Technical Data 52-365, Westinghouse Electric Corporation, Materials Manufacturing Division, Blairsville, Penn. 1963.

TABLE 1

Summary of Liquid Alkali Metal Analysis

Sample	Time Taken	Date	Time Liquid Al. Metal Held in Retort	Box O_2 ppm	Box H_2O ppm	Liquid Alkali Metal Temp ^{o}F	Oxide* Impurity ppm
1	3:20 pm	7/28/66	0	4	20	300	6
2	4:50 pm	7/28/66	1-1/2 hr	1.5	15	300	6
3	6:21 pm	7/28/66	3 hr	3	19	300	7
4	7:50 pm	7/28/66	4-1/2 hr	6	70	300	5
5	4:45 pm	9/6/66	4 days	39	105	400	8
8	4:50 pm	10/7/66	5 days	18	1.1	500	18
12	4:00 pm	12/9/66	7 days	56	0.4	400	7
13	4:30 pm	12/22/66	13 days	1.0	0.2	400	7
14	4:35 pm	1/16/67	17 days	5.2	3.0	600	26 Ⓐ
15	2:55 pm	3/1/67	15 days	2.0	0.5	450	10

* Unamalgamated residue calculated as oxygen from K_2O.

Ⓐ After box back filled with air during overnight power failure.

TABLE 2

Nominal Chemical Composition of Alloys Used in Cavitation Damage Studies in Liquid Potassium
(Weight Percent*)

Metal	Cr	Ni	Mo	Mn	Si	C	P	S	Fe
316 Stainless Steel	16-18	11-14	2-3	2.0	0.75	0.08	0.03	0.03	Bal.

T-111	W	Hf	Ta	Cb	Mo	O	Fe	C
	7.87	2.03	Bal.	110 ppm	110 ppm	25 ppm	20 ppm	10 ppm
	N	H	Ni	V	Co			
	10 ppm	10 ppm	10 ppm	10 ppm	10 ppm			

TZC (1)	Ti	Zr	C	Mo
	1.36	0.36	0.095	Bal.

Cb-132M (2)	Ta	W	Mo	Zr	C	Cb	Cu	Cr	Mn	V
	19.81	15.01	5.07	2.17	0.15	Bal.	750 ppm	720 ppm	710 ppm	710 ppm
	Ni	Ti	Al	Mg	Fe	N_2	Si	H_2	O_2	
	710 ppm	710 ppm	710 ppm	72 ppm	35 ppm	26-28 ppm	15 ppm	4.1 ppm	4 ppm	

Ti + 10% Cb Binder	90%	10%

* Except where otherwise specified.

(1) Stress Relieved - 2200°F for 1/2 hour (v.c.) (vacuum cooled)
Recrystallized - 3400°F for 1 hour (v.c.)
(2) Stress Relieved - 2200°F for 1 hour (v.c.)
Recrystallized - 2700°F for 1 hour (v.c.)

TABLE 3

Some Mechanical Properties of Alloys Under Test
(Room Temperature)

Material	Yield Strength (psi)	Tensile Strength (psi)	Elongation in 2"* %
T-111	73,000	89,600	(in 1") 42
Cb-132M	109,800	121,200	4.2
316 Stainless Steel	68,000	91,400	36
Class A	60,000 90,000	80,000- 110,000	(in 4D) 5
TZC Class B**	100,000- 140,000	125,000- 175,000	(in 4D) 15
TiC + 10% Cb Binder	Not yet available		

* Except where otherwise specified.
** Parallel to direction of work.

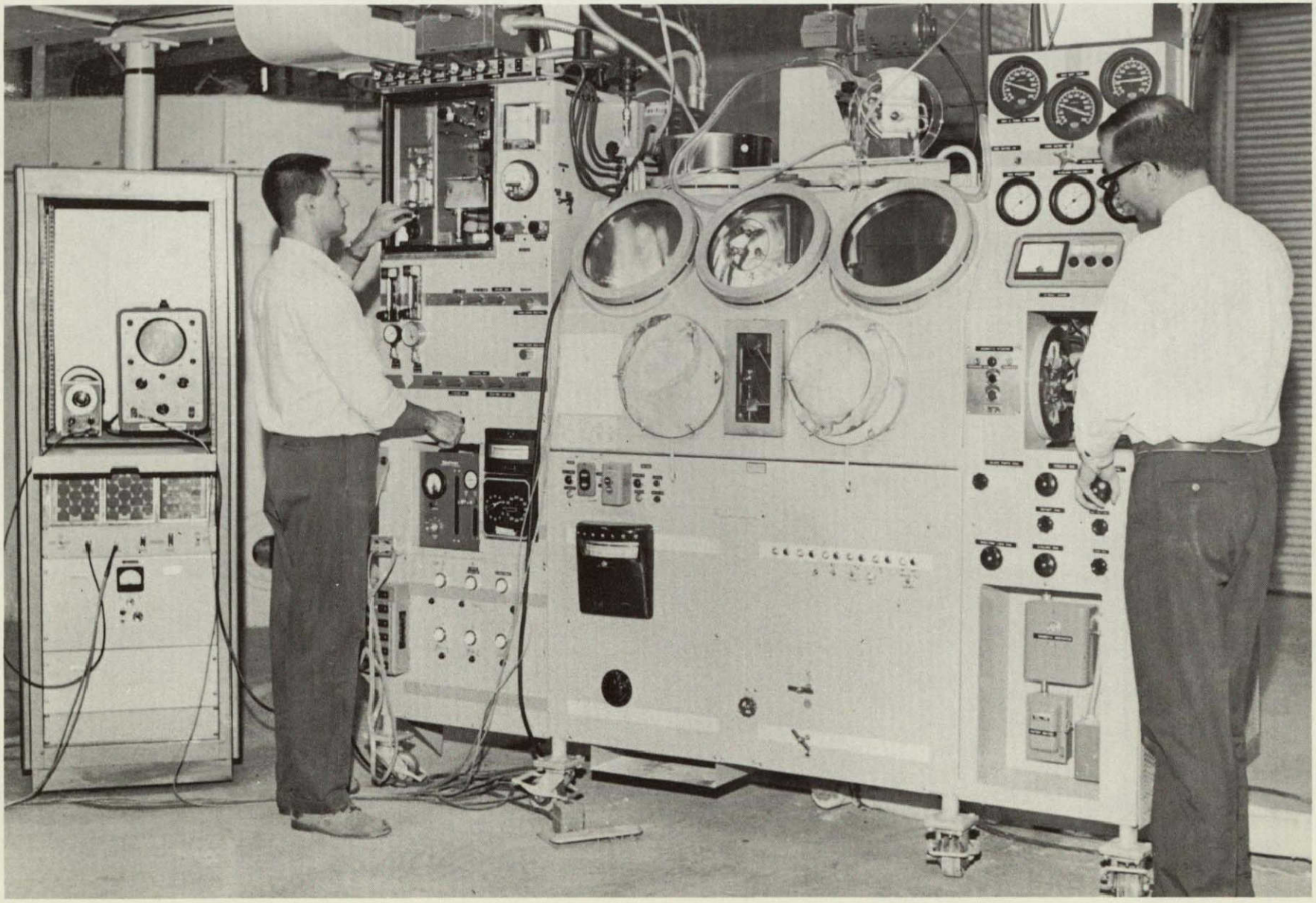

FIGURE 1 - OVERALL VIEW OF DRY BOX FACILITY

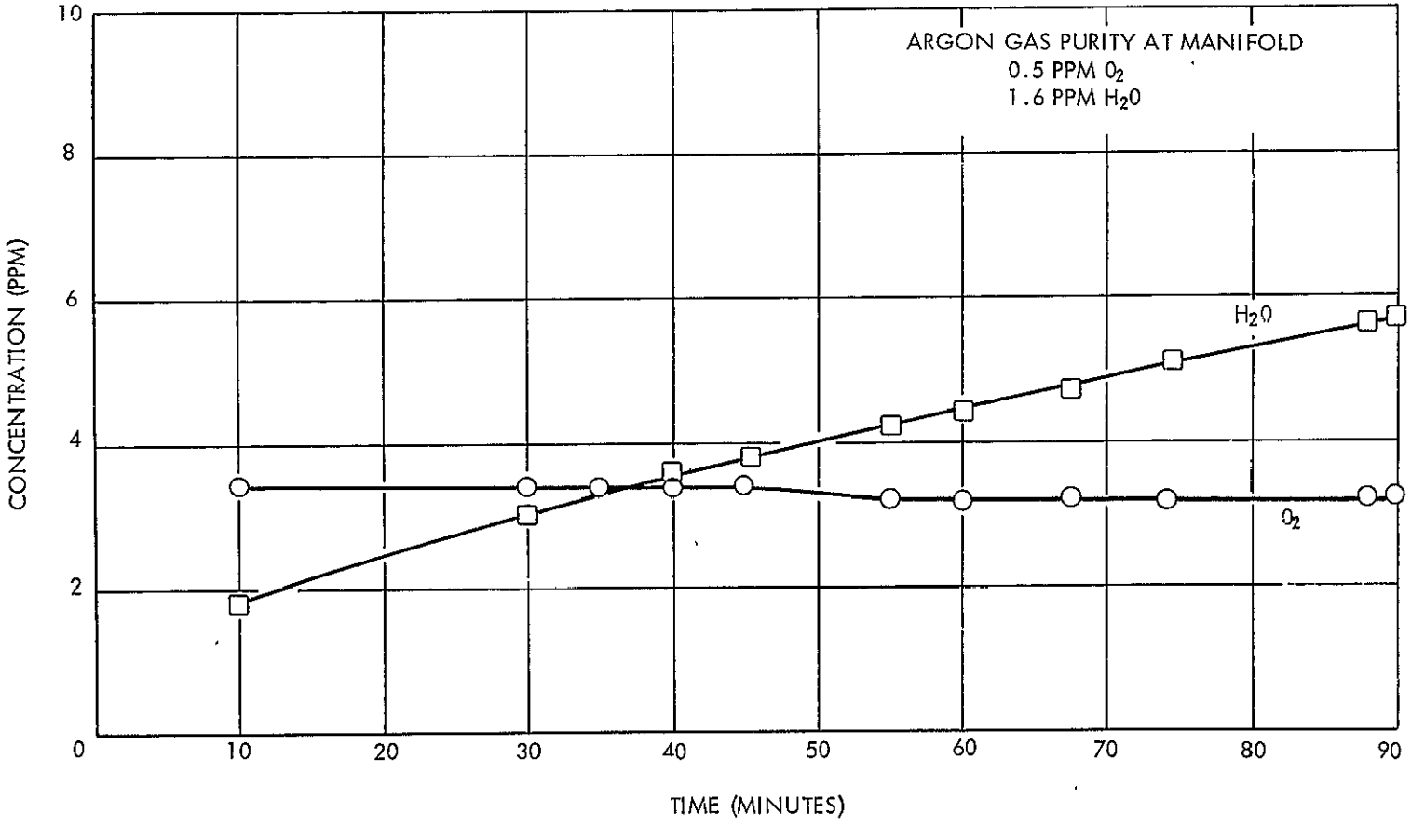

FIGURE 2 - RISE OF O_2 AND H_2O IN BOX COVER GAS (GLOVE PORT COVERS CLOSED)

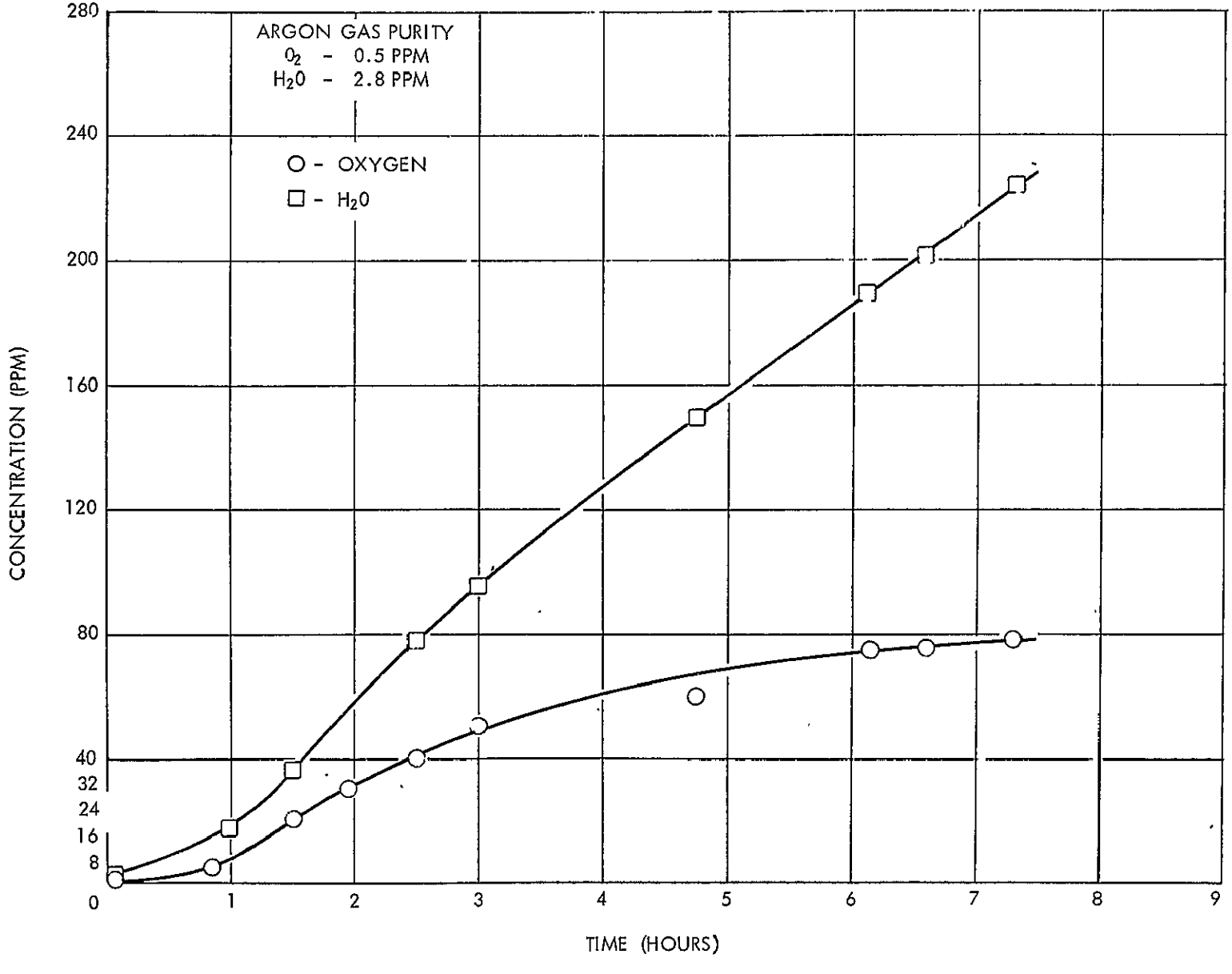

FIGURE 3 - RISE OF O_2 AND H_2O IN BOX COVER GAS (GLOVE PORT COVERS OPEN)

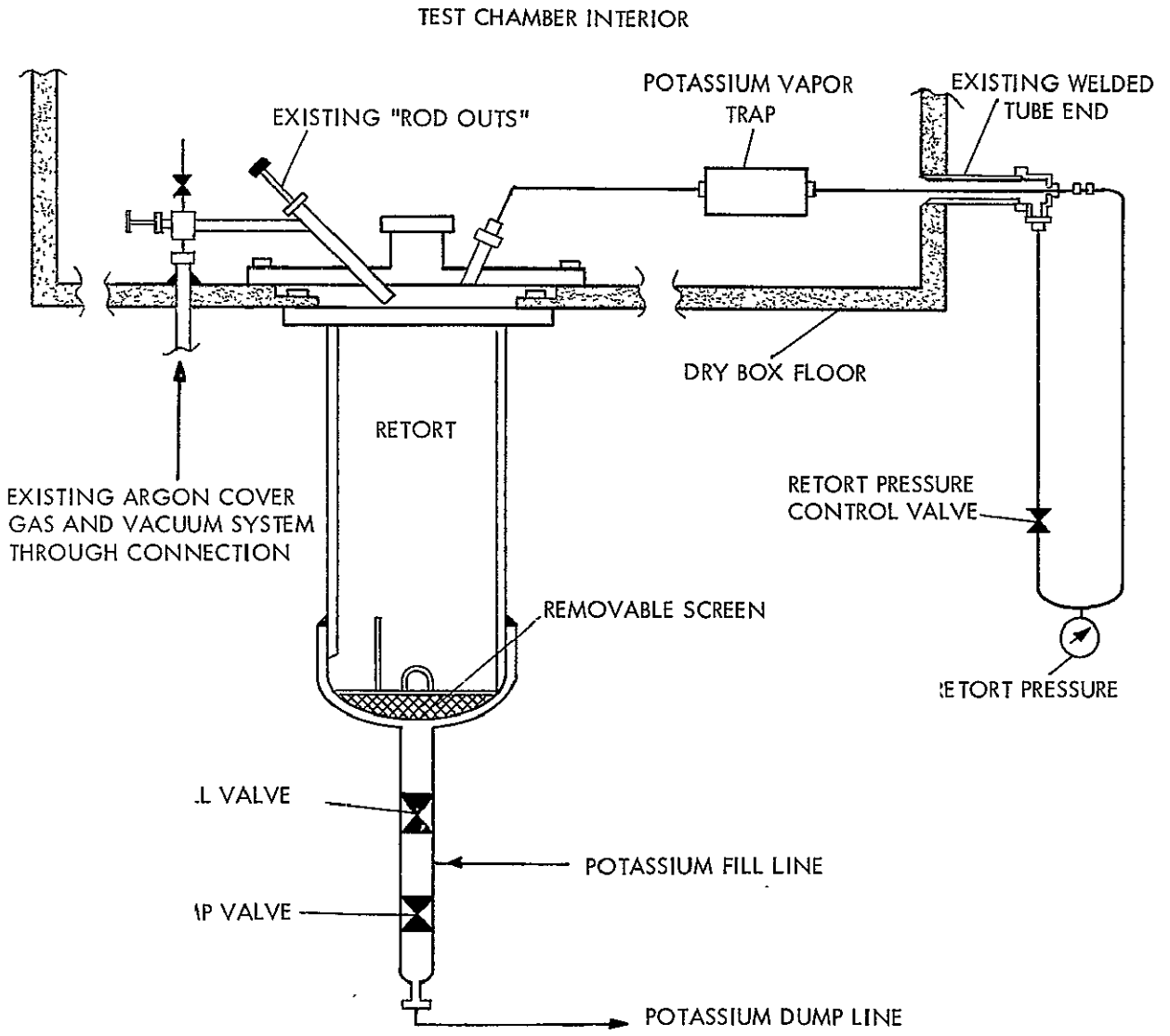

FIGURE 4 - MODIFIED RETORT SYSTEM

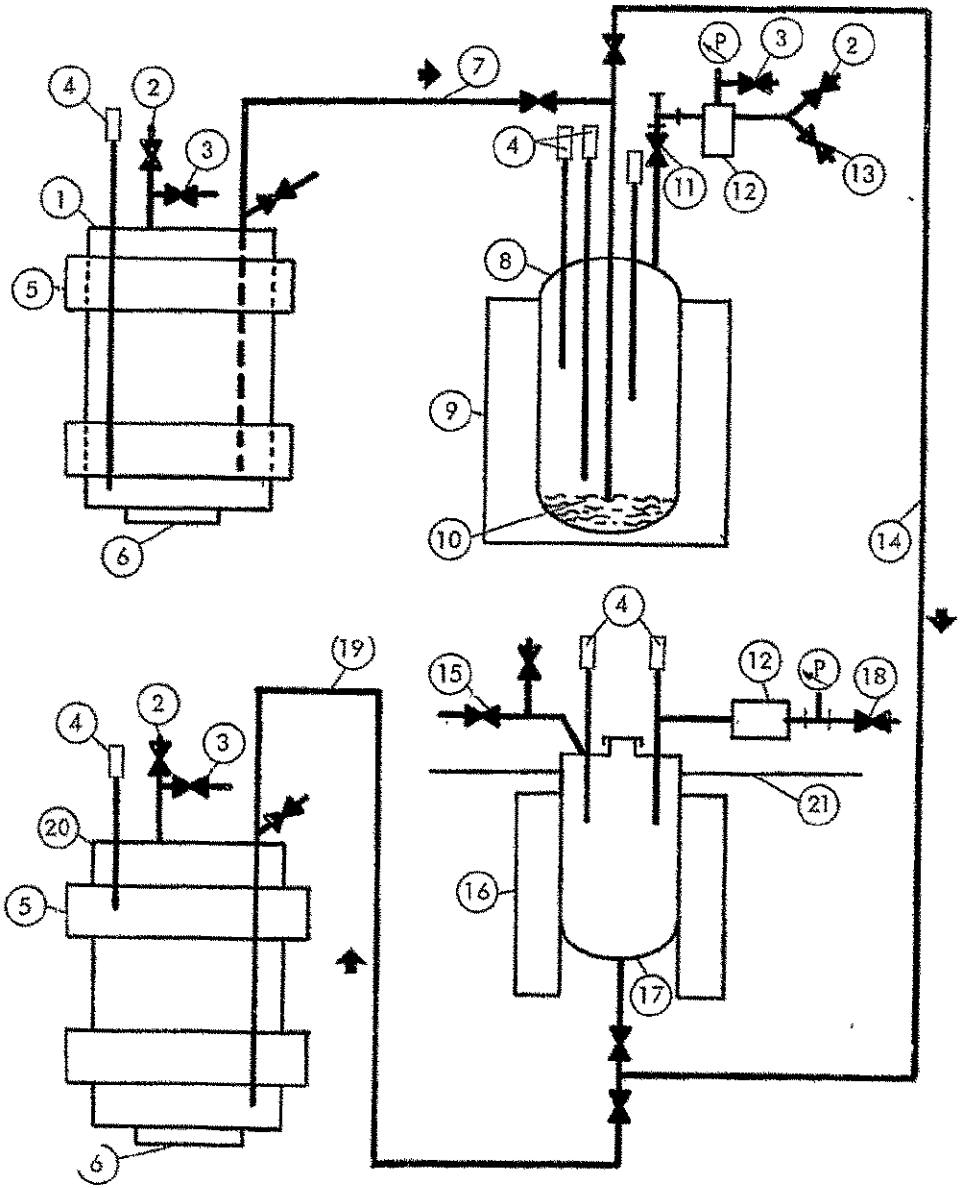

1. POTASSIUM FILL DRUM (30 GALLONS)
2. COVER GAS INLET
3. PURGE AND HIGH PRESSURE RELIEF
4. THERMOCOUPLES
5. BAND HEATERS
6. RING HEATERS
7. POTASSIUM CHARGE LINE
8. POTASSIUM HOT TRAP
9. HOT TRAP FURNACE
10. ZIRCONIUM CHIPS (GETTERING MATERIAL)
11. BALL VALVE
12. POTASSIUM VAPOR TRAP
13. VACUUM INLET
14. POTASSIUM FILL LINE
15. COVER GAS, VACUUM AND GAGE LINE
16. RETORT FURNACE
17. RETORT
18. RETORT PRESSURE CONTROL
19. POTASSIUM DRAIN LINE
20. POTASSIUM DUMP DRUM (30 GALLONS)
21. DRY BOX FLOOR

FIGURE 5 - SCHEMATIC POTASSIUM METAL LOOP FOR CAVITATION DAMAGE FACILITY

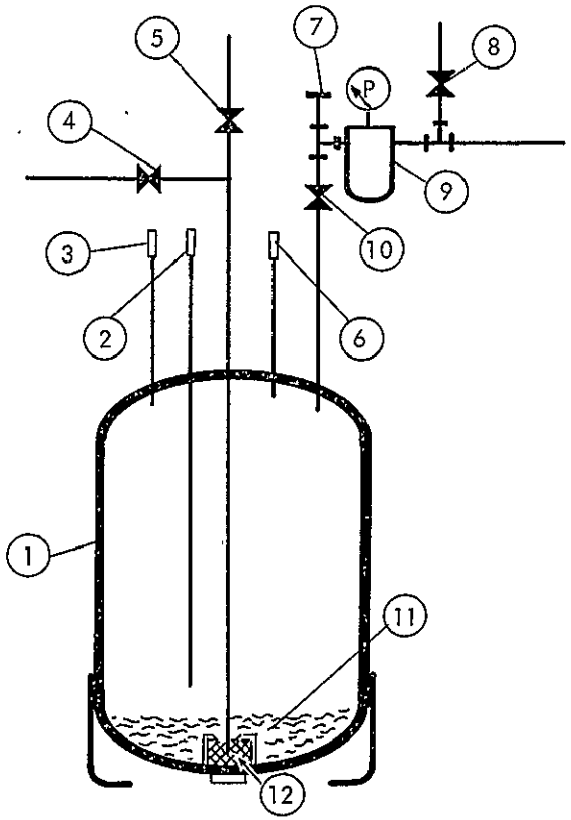

1. HOT TRAP BODY
2. LOW LEVEL INDICATOR THERMOCOUPLE
3. HIGH LEVEL INDICATOR THERMOCOUPLE
4. POTASSIUM CHARGE VALVE
5. POTASSIUM FILL VALVE
6. HIGH TEMPERATURE FURNACE CUTOFF T.C.
7. ROD-OUT SYSTEM
8. ARGON PURGE AND RELIEF
9. VAPOR TRAP
10. 1" BALL VALVE TO ISOLATE COMPONENTS ABOVE WHILE HOT TRAPPING
11. ZIRCONIUM CHIPS
12. WIRE MESH STRAINER AROUND DIP TUBE

FIGURE 6 - SCHEMATIC POTASSIUM HOT TRAP

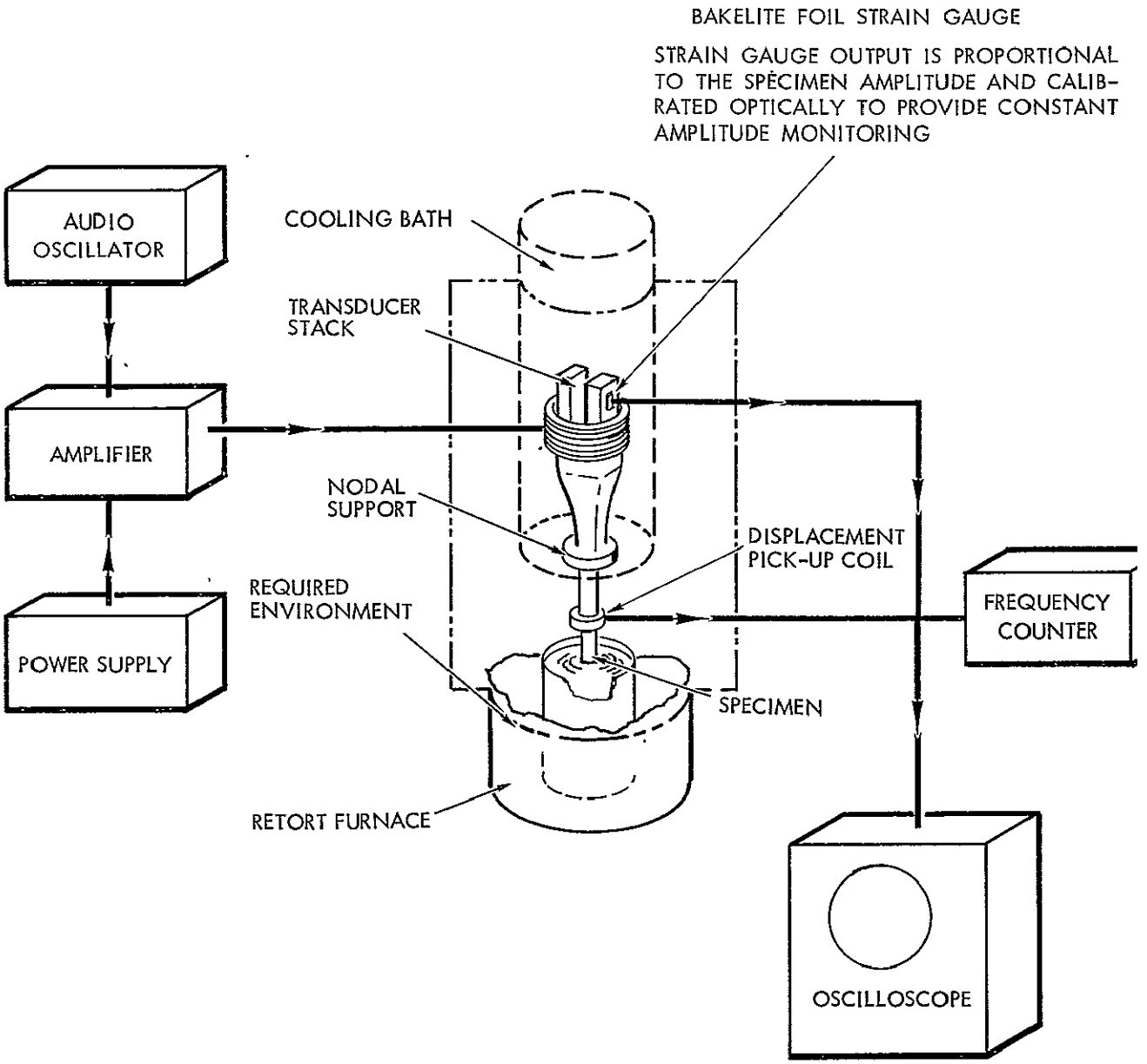

FIGURE 7 - BLOCK DIAGRAM OF THE MAGNETOSTRICTION APPARATUS USED FOR CAVITATION DAMAGE TESTS AND FOR HIGH FREQUENCY FATIGUE TESTS

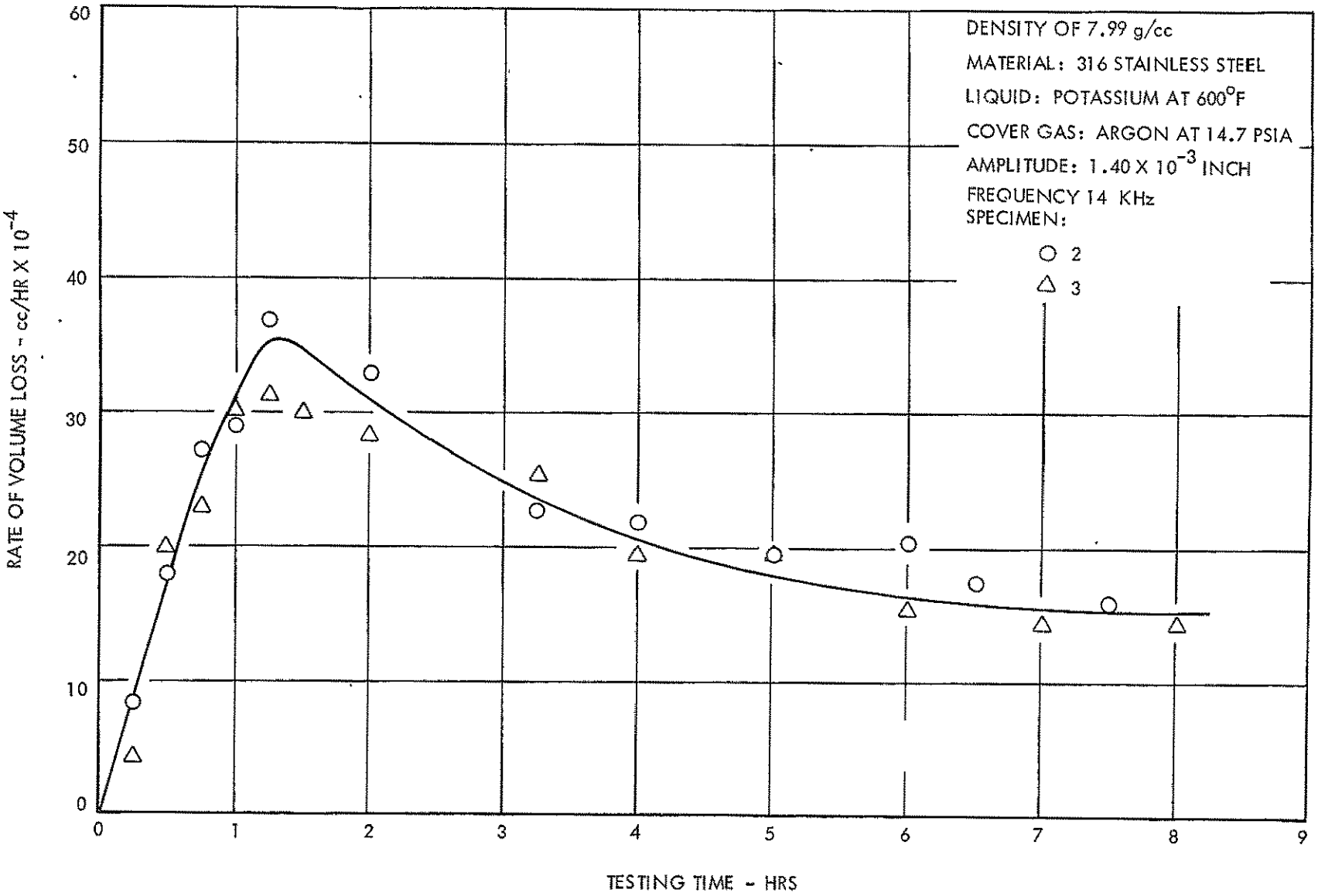

FIGURE 8 - THE EFFECT OF TESTING TIME ON THE CAVITATION DAMAGE RATE OF 316 STAINLESS STEEL IN LIQUID POTASSIUM

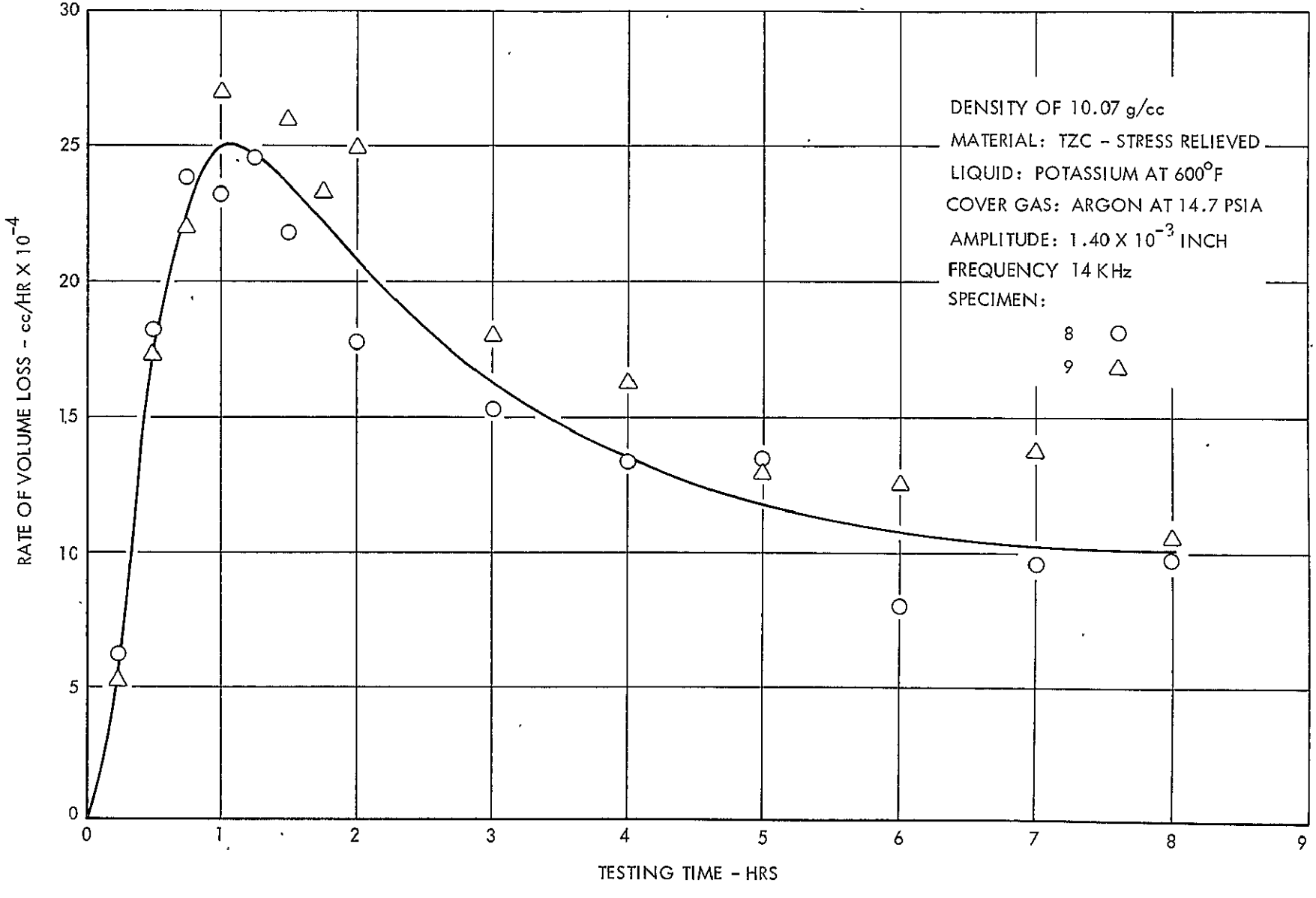

FIGURE 10 - EFFECT OF TESTING TIME ON THE CAVITATION DAMAGE RATE OF TZC IN LIQUID POTASSIUM

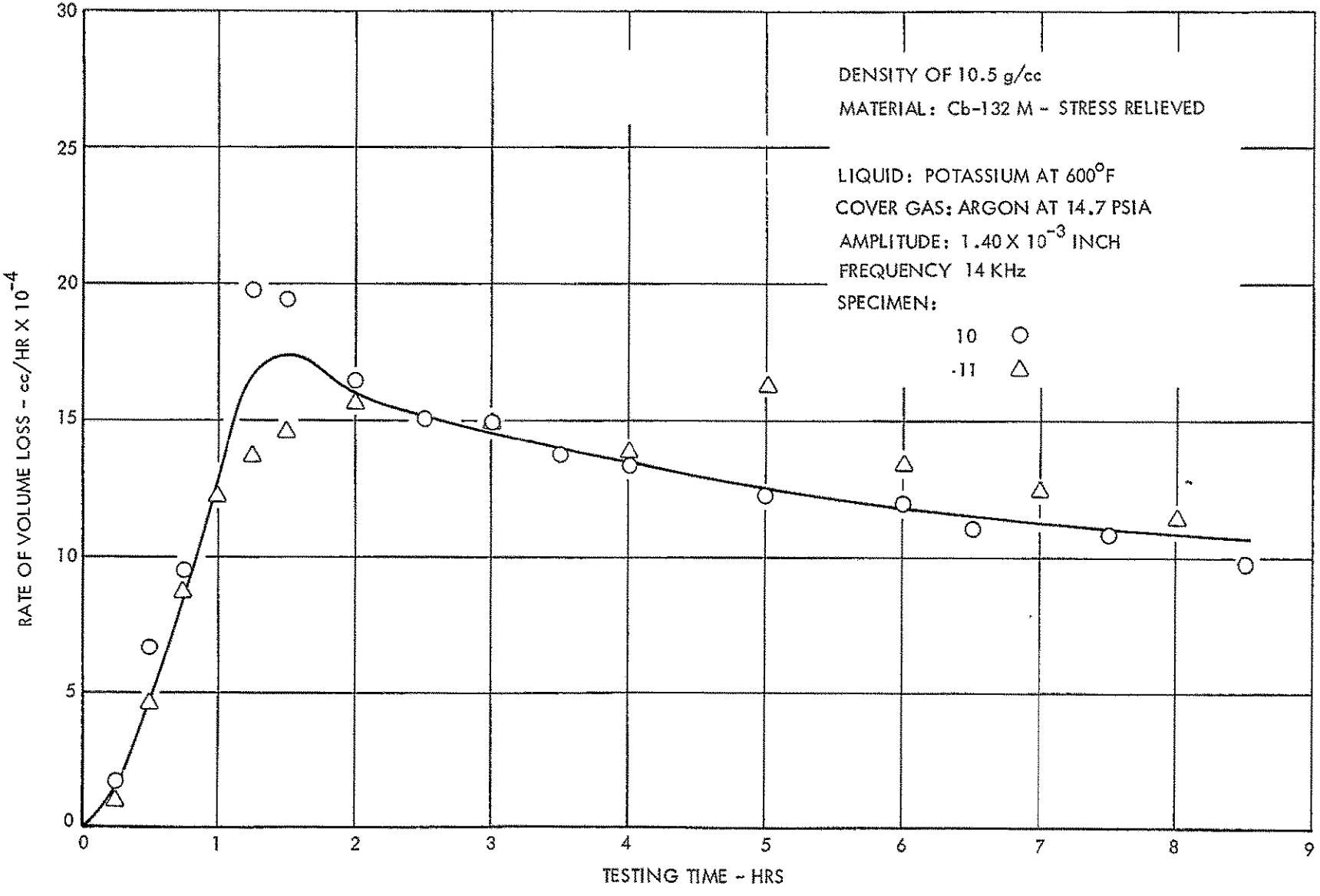

FIGURE 11 - EFFECT OF TESTING TIME ON THE CAVITATION DAMAGE RATE OF Cb-132 M IN LIQUID POTASSIUM

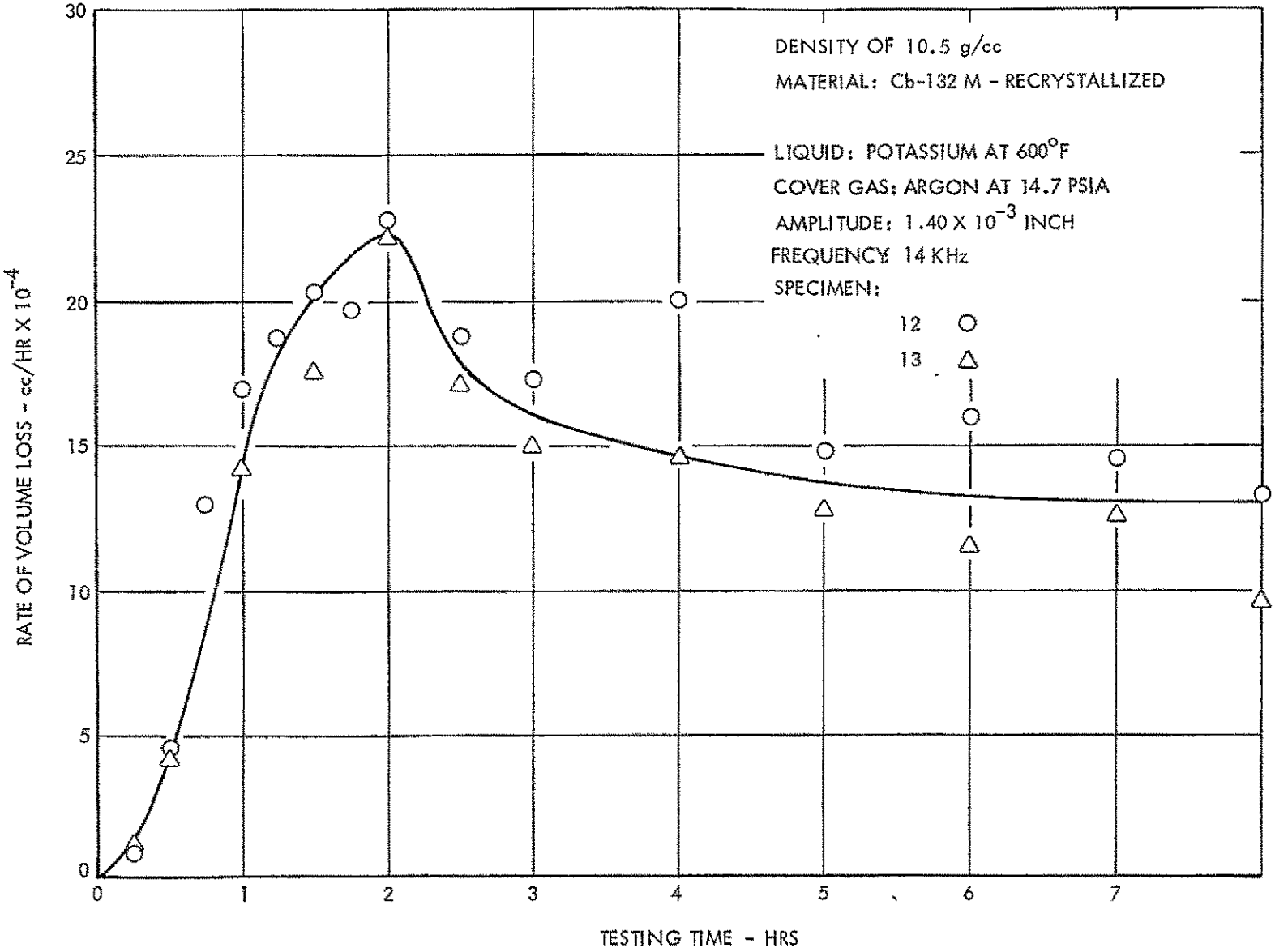

FIGURE 12 - EFFECT OF TESTING TIME ON THE CAVITATION DAMAGE RATE OF Cb-132 M IN LIQUID POTASSIUM

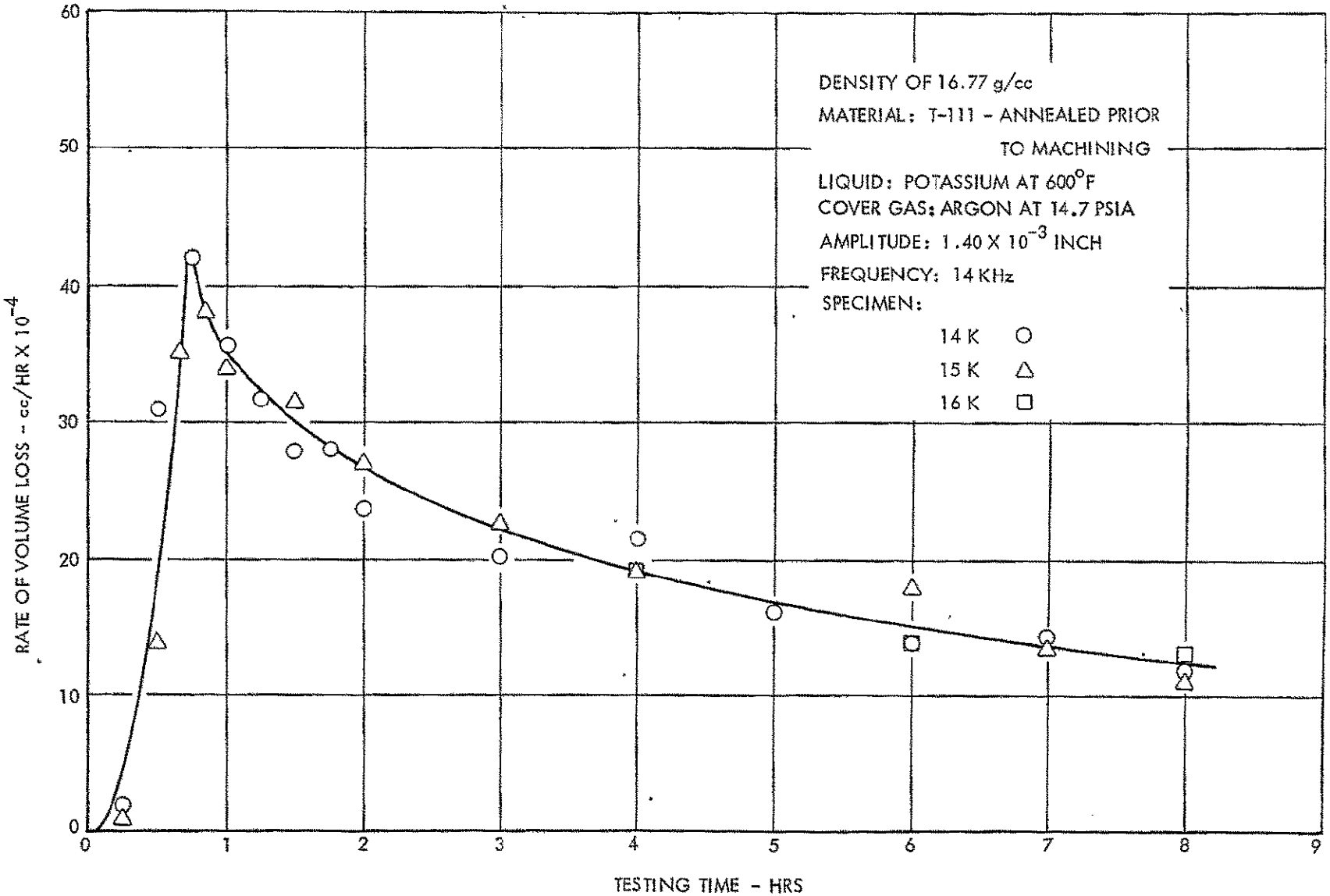

FIGURE 13 - EFFECT OF TESTING TIME ON THE CAVITATION DAMAGE RATE OF T-111 IN LIQUID POTASSIUM

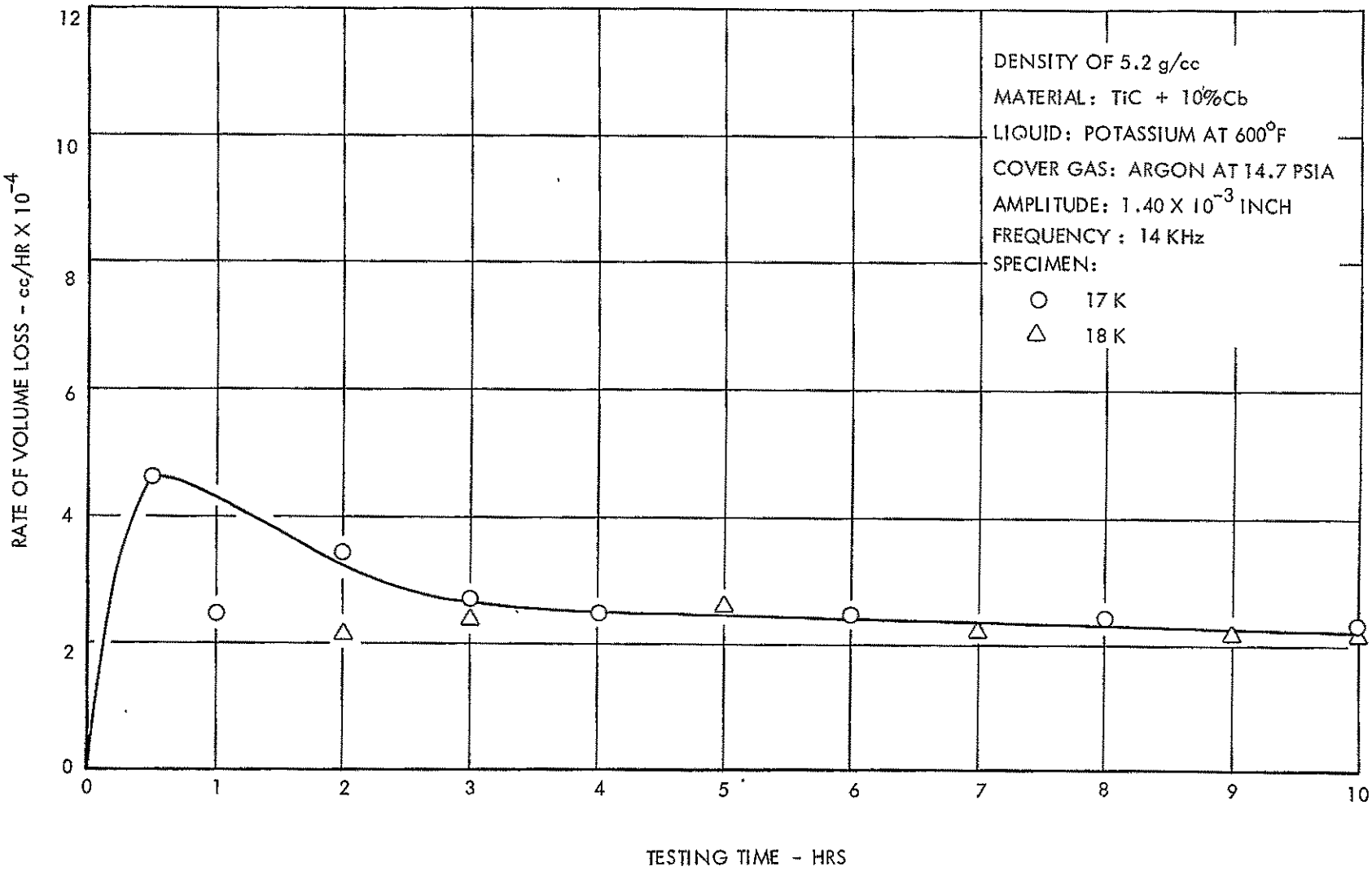

FIGURE 14 - THE EFFECT OF TESTING TIME ON THE CAVITATION DAMAGE RATE OF TiC + 10% Cb IN LIQUID POTASSIUM

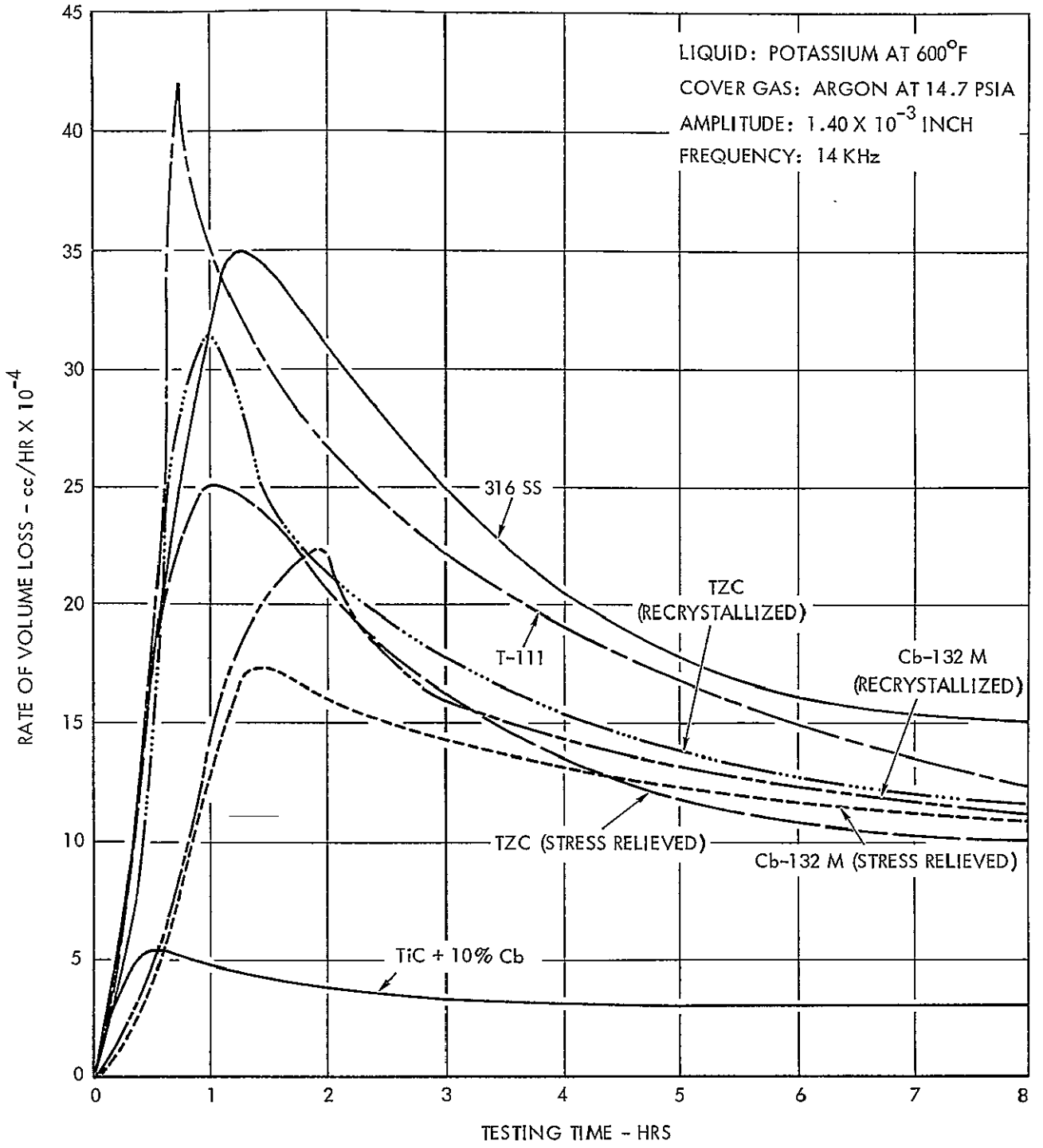

FIGURE 15 - COMPARATIVE CAVITATION DAMAGE RESISTANCE OF REFRACTORY ALLOYS IN HIGH TEMPERATURE LIQUID POTASSIUM

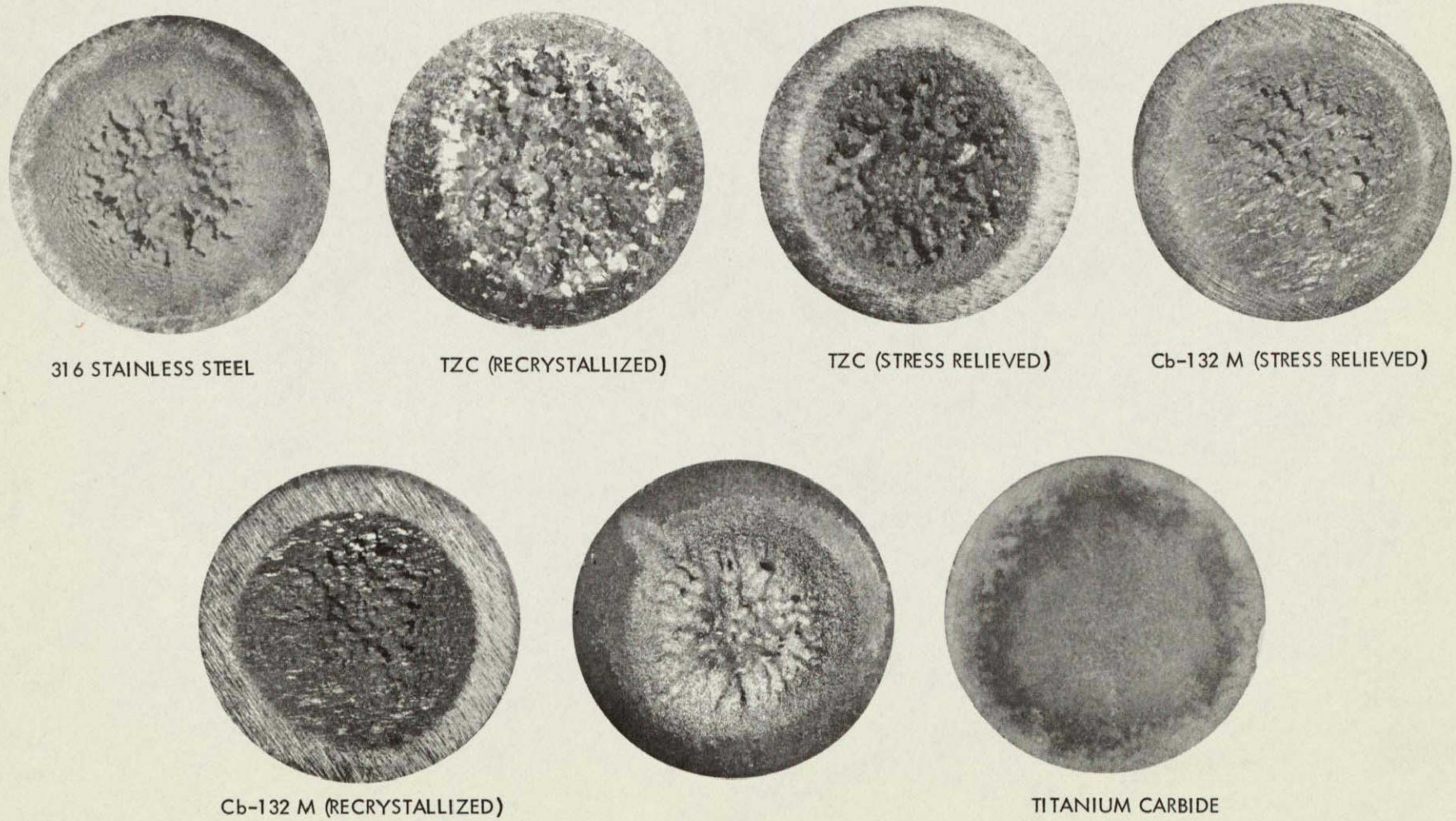

FIGURE 16 - APPEARANCE OF ERODED SURFACE OF ALL MATERIALS TESTED UNDER THIS PROGRAM

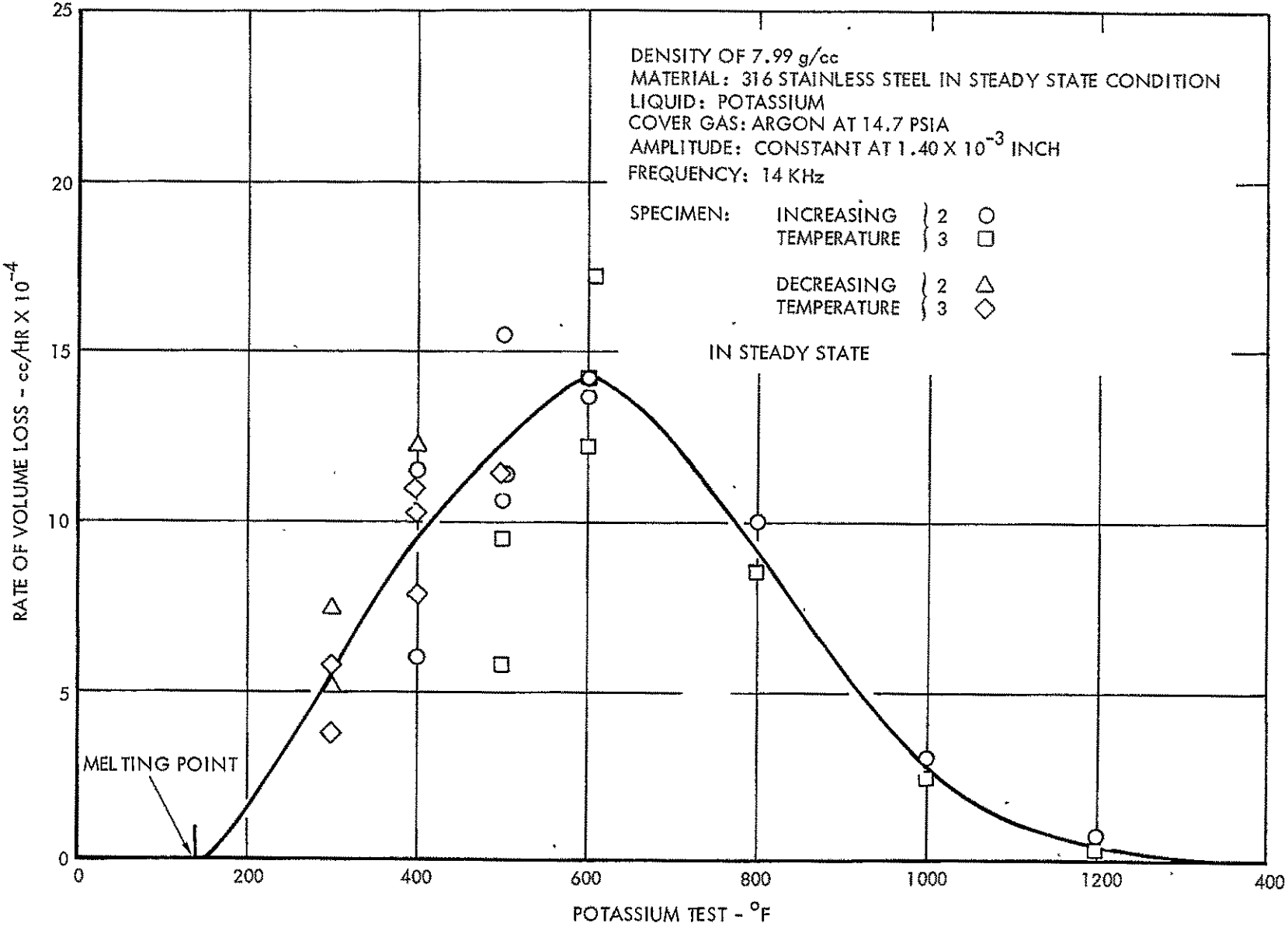

FIGURE 17 - EFFECT OF TEMPERATURE ON THE CAVITATION DAMAGE RATE OF 316 STAINLESS STEEL IN LIQUID POTASSIUM

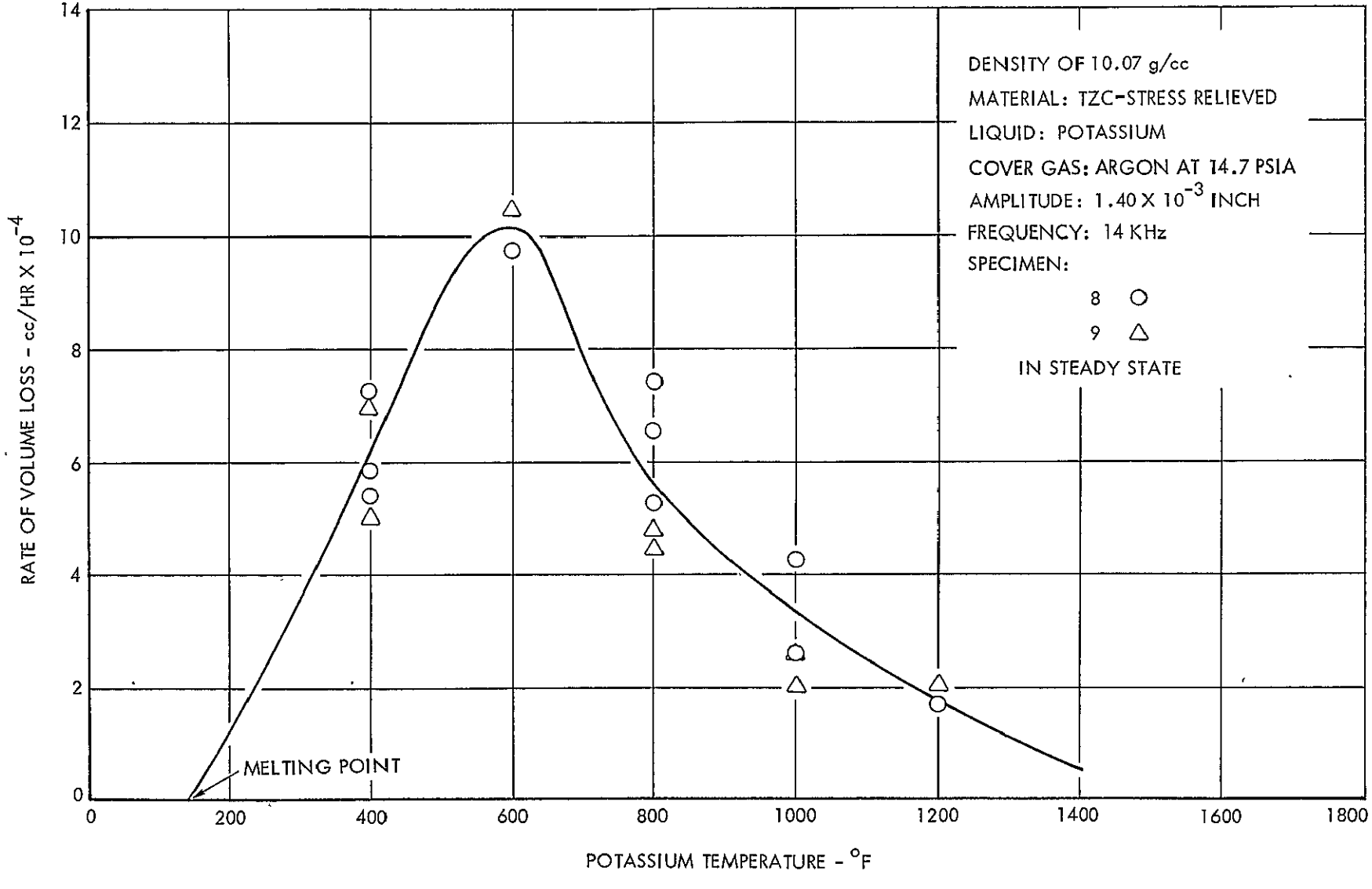

FIGURE 18 - EFFECT OF TEMPERATURE ON THE CAVITATION DAMAGE RATE OF TZC IN LIQUID POTASSIUM

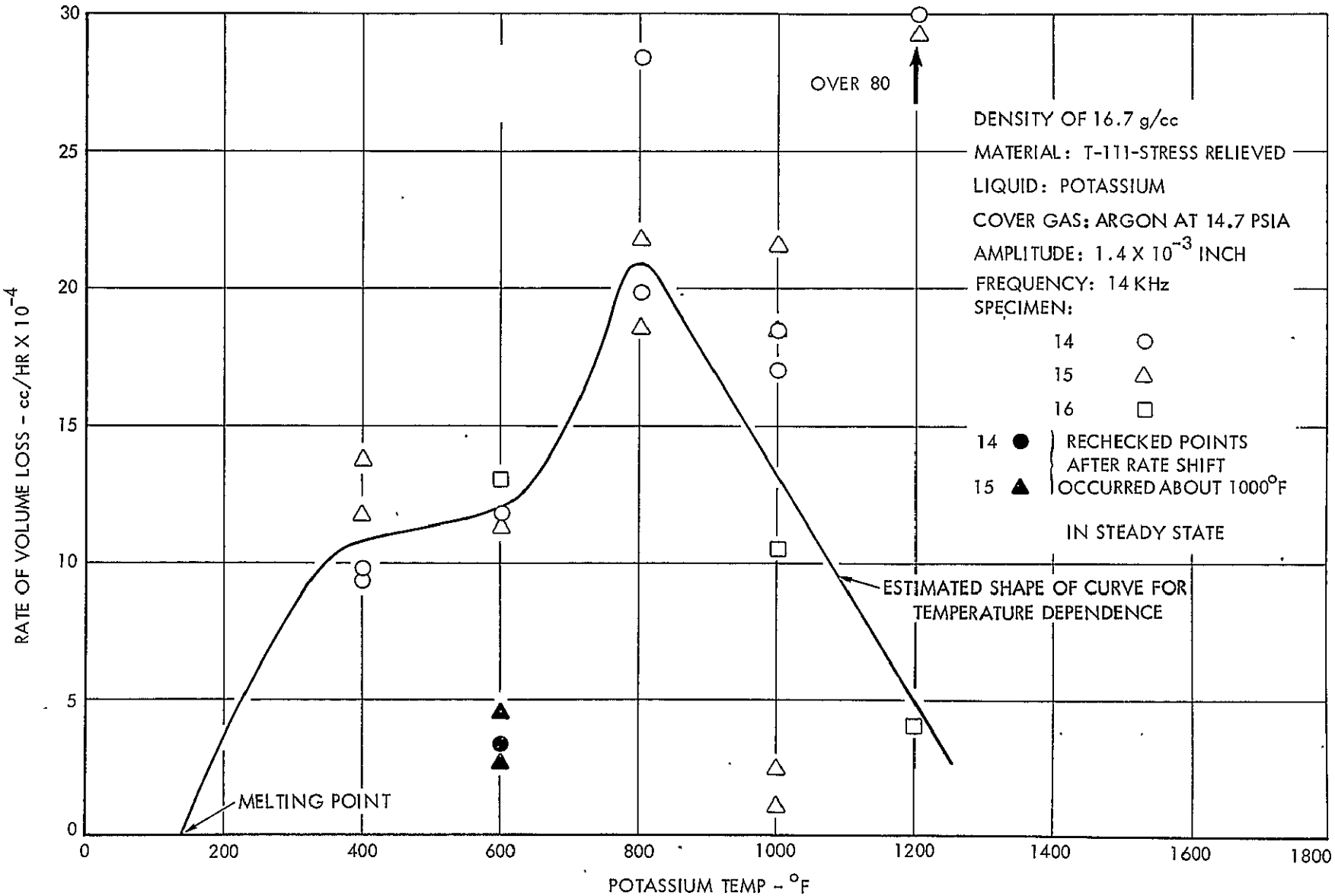

FIGURE 19 - EFFECT OF TEMPERATURE ON THE CAVITATION DAMAGE RATE OF T-111 IN LIQUID POTASSIUM

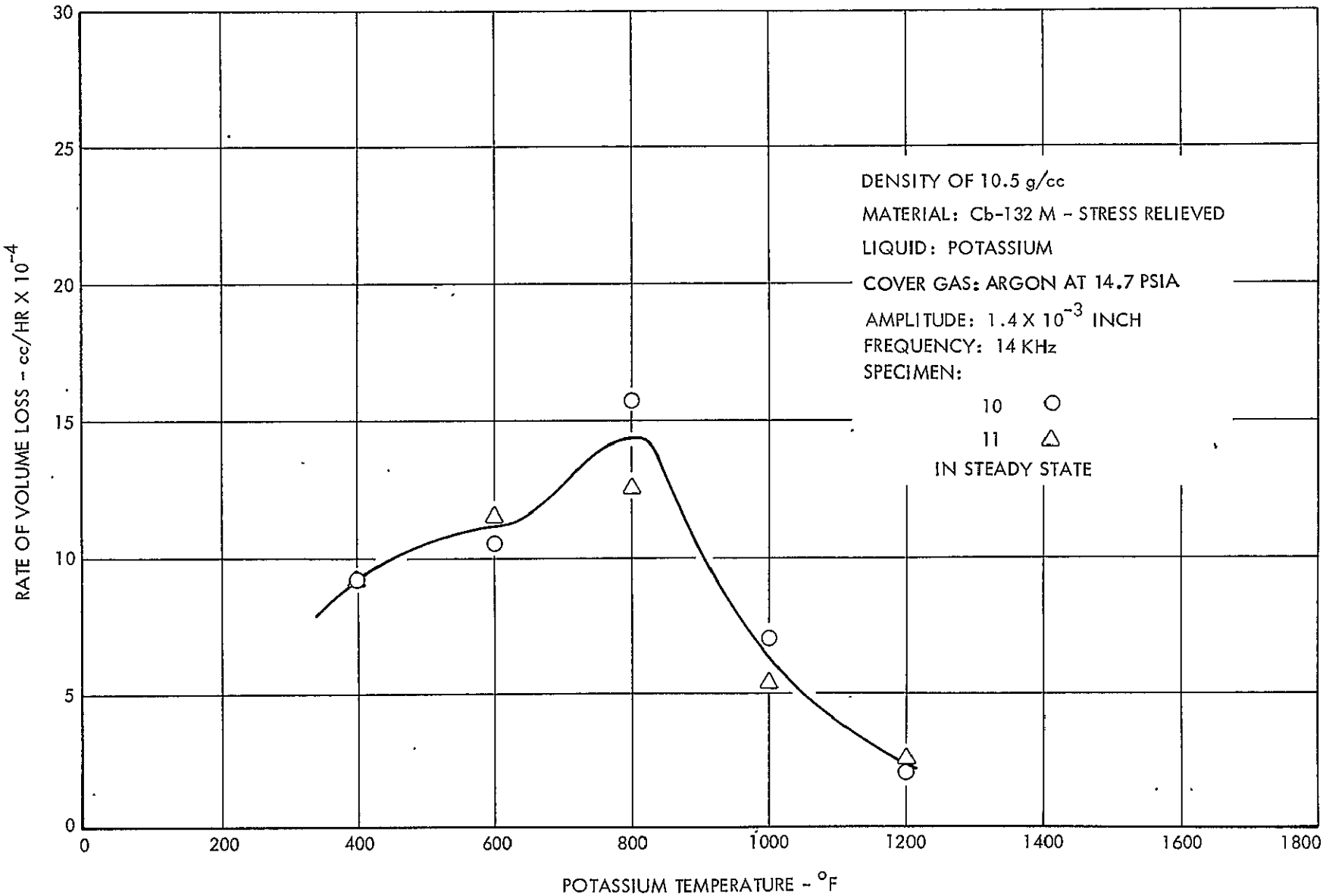

FIGURE 20 - EFFECT OF TEMPERATURE ON THE CAVITATION DAMAGE RATE OF Cb-132 M IN LIQUID POTASSIUM

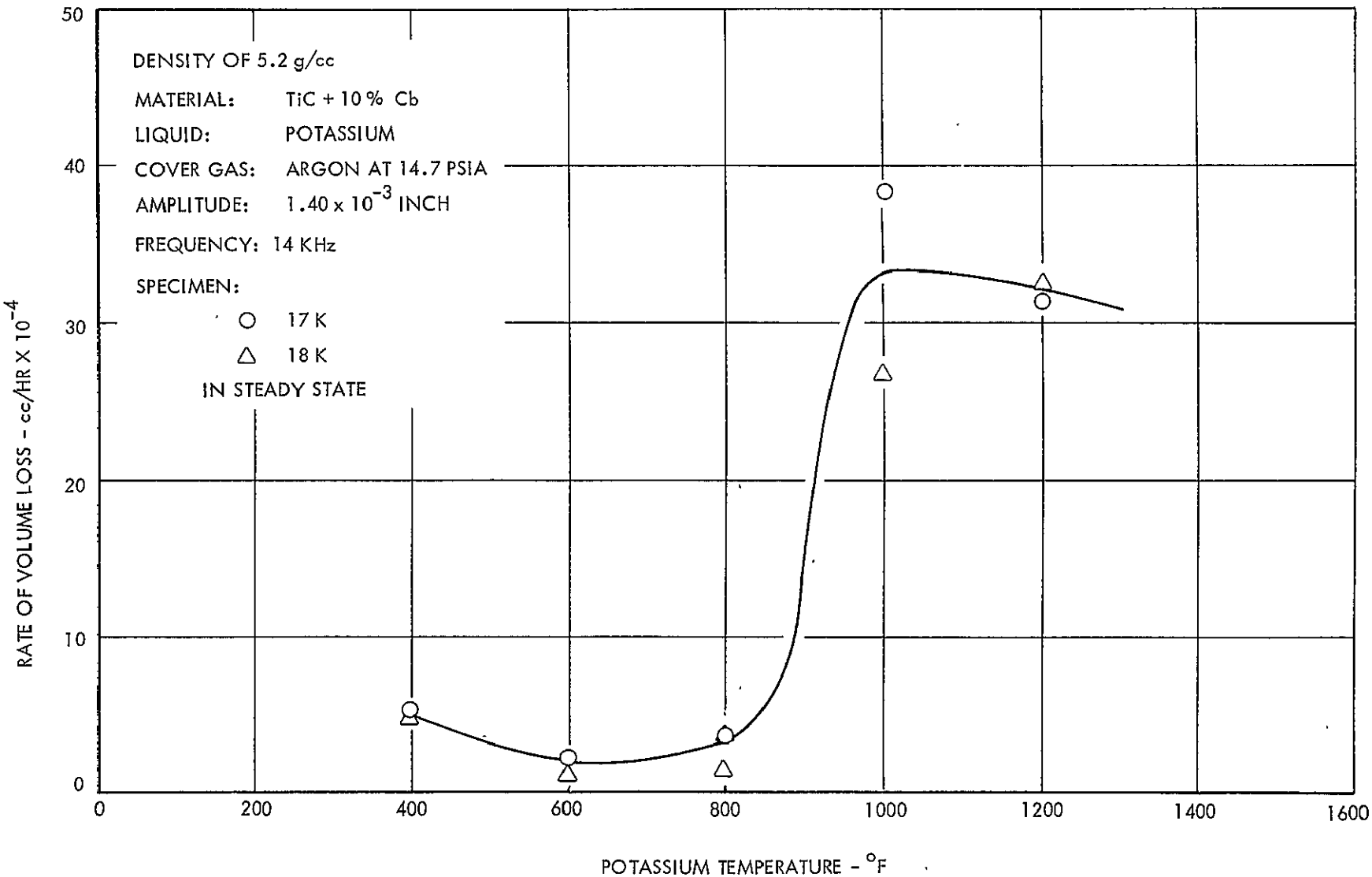

FIGURE 21 - THE EFFECT OF TEMPERATURE ON THE CAVITATION DAMAGE RATE OF TiC + 10% Cb IN LIQUID POTASSIUM

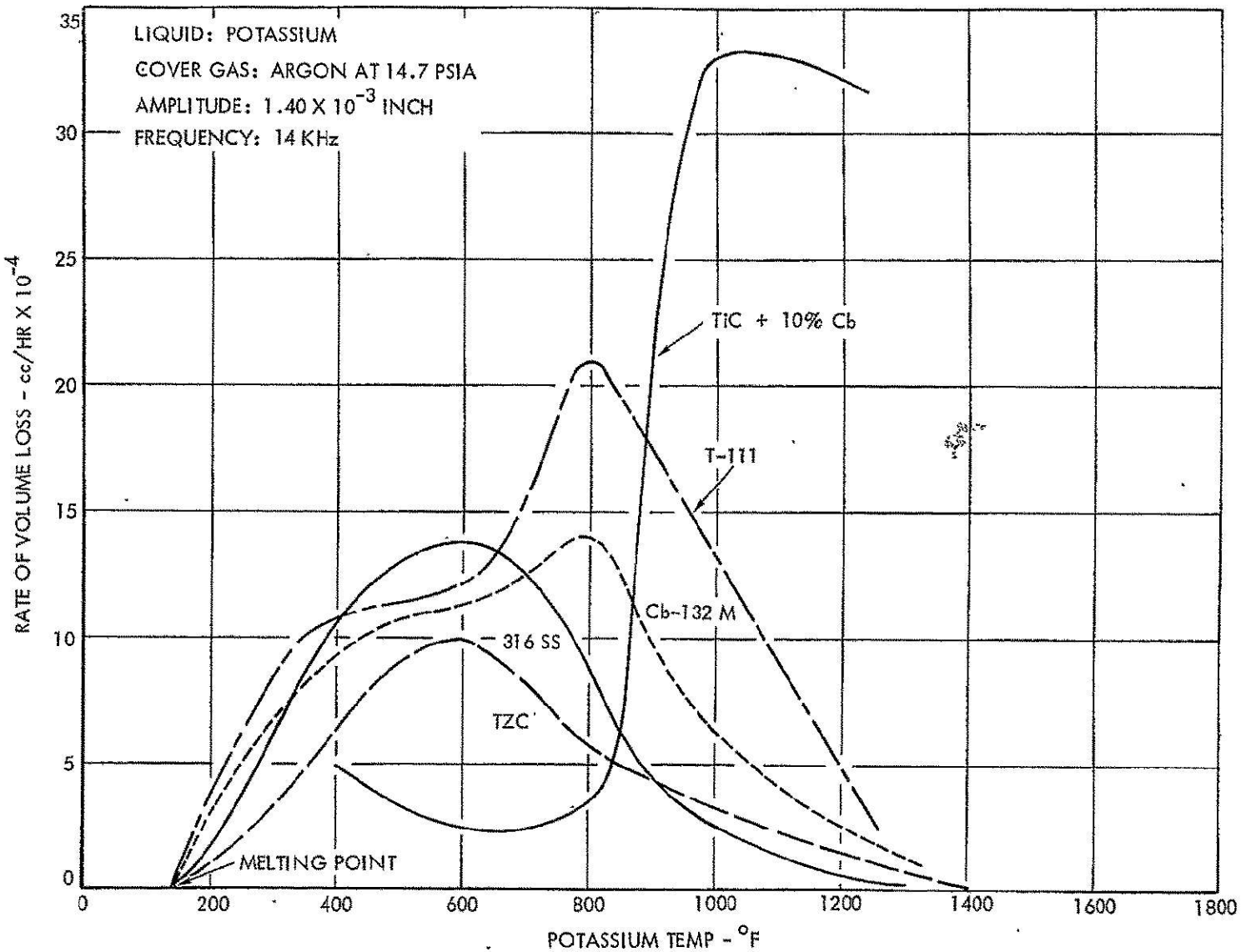

FIGURE 22 - COMPARISON OF THE EFFECT OF TEMPERATURE ON THE CAVITATION DAMAGE RATES OF REFRACTORY ALLOYS IN LIQUID POTASSIUM

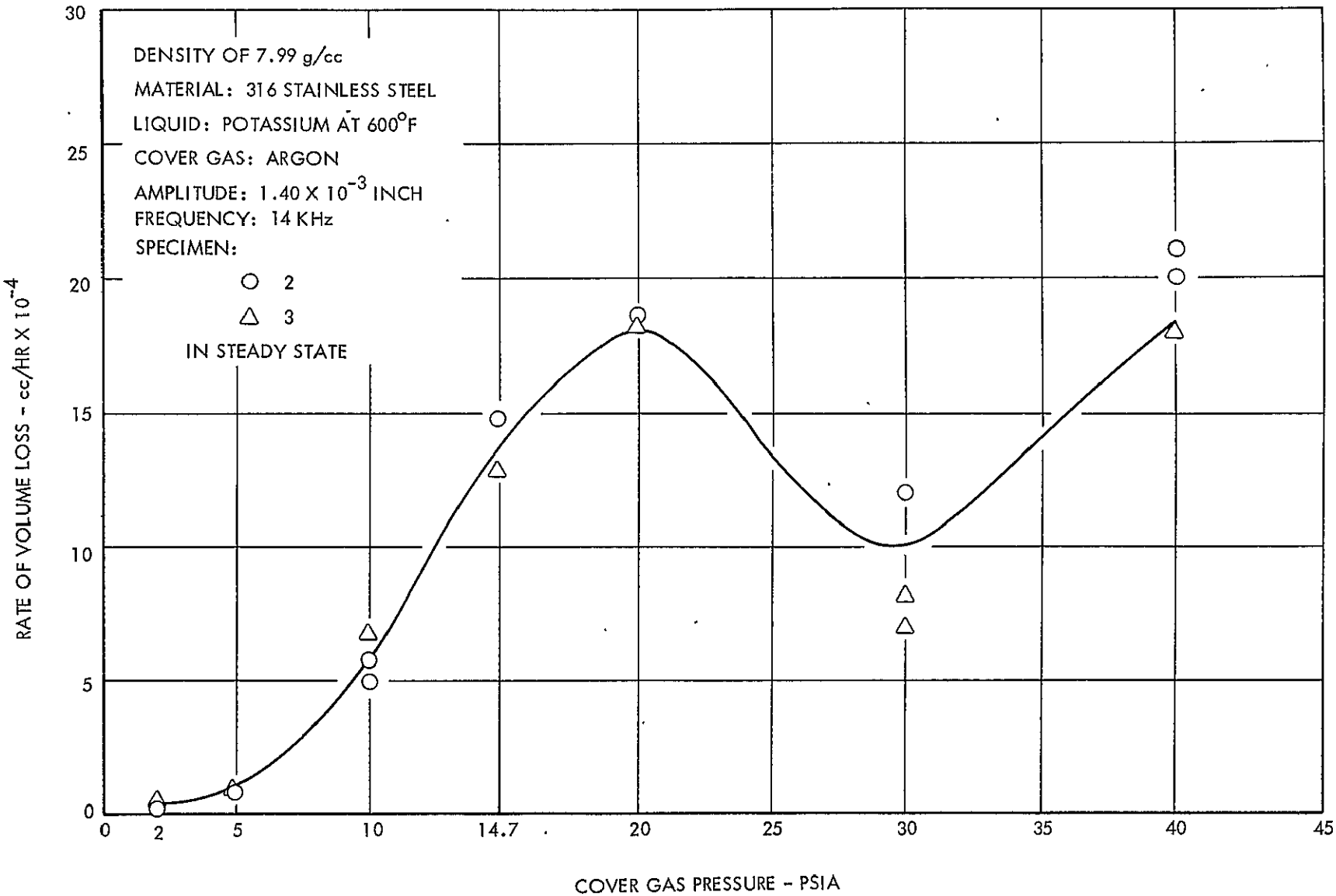

FIGURE 23 - THE EFFECT OF PRESSURE ON THE CAVITATION DAMAGE RATE OF 316 STAINLESS STEEL IN LIQUID POTASSIUM

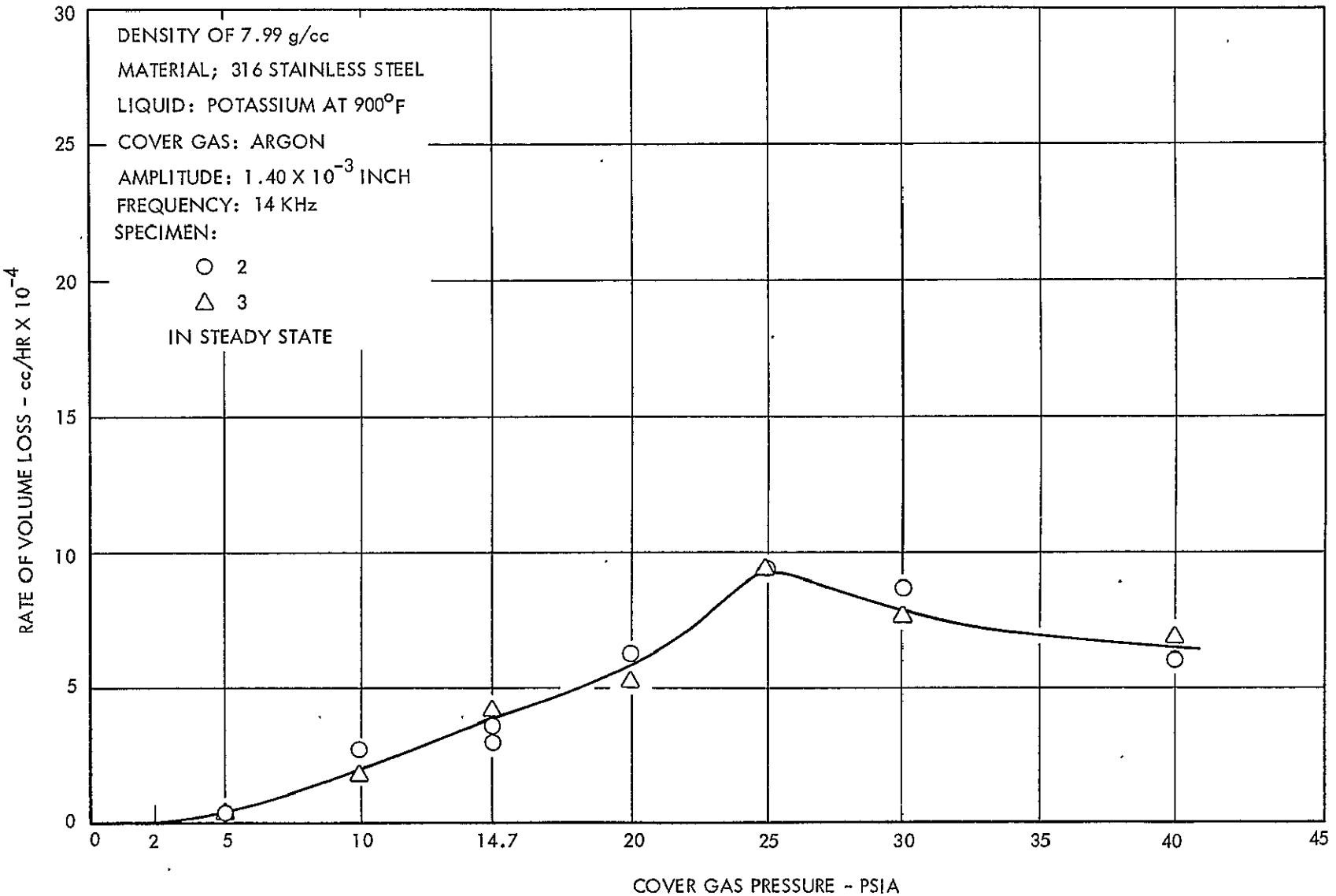

FIGURE 24 - THE EFFECT OF PRESSURE ON THE CAVITATION DAMAGE RATE OF 316 STAINLESS STEEL IN LIQUID POTASSIUM

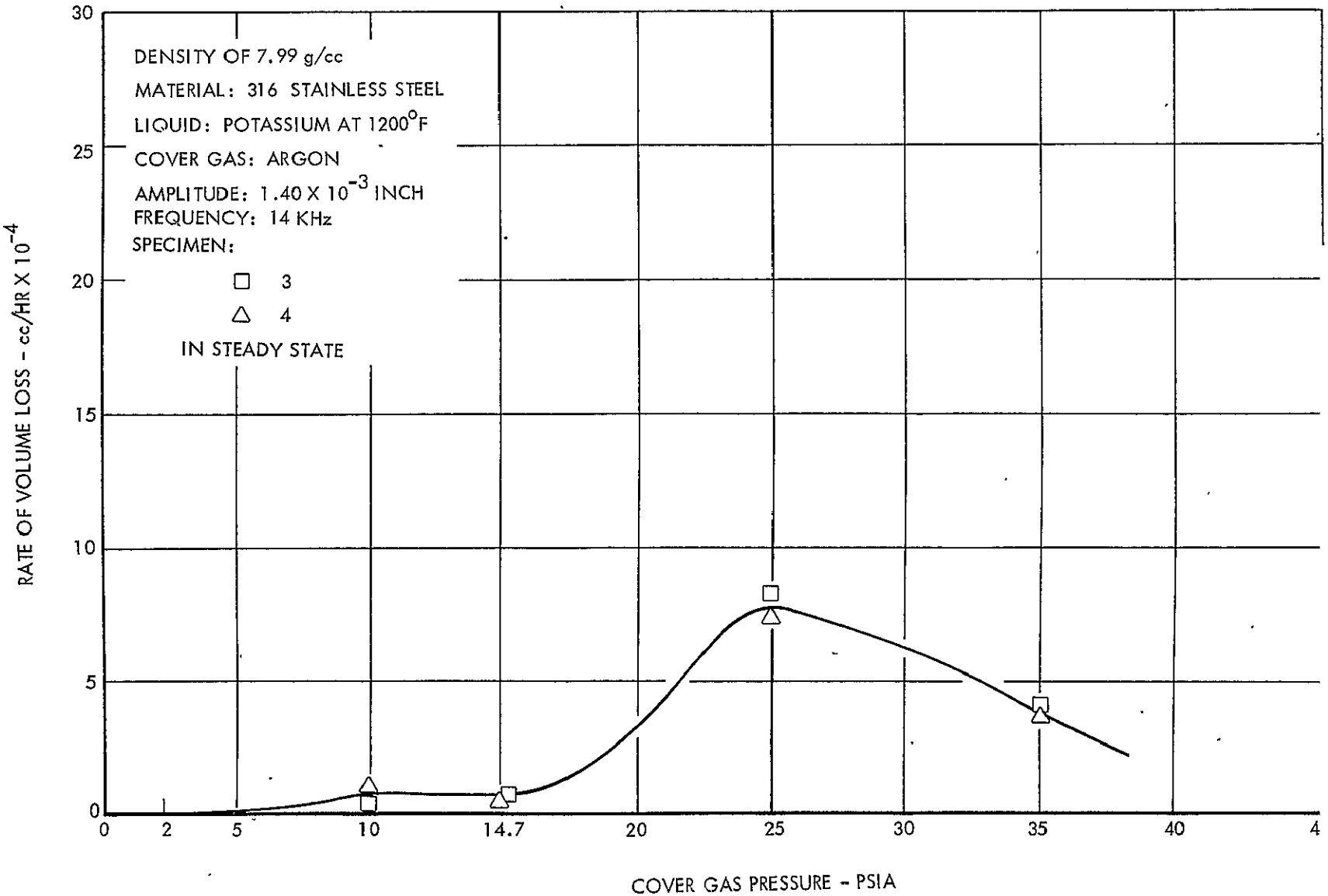

FIGURE 25 - THE EFFECT OF PRESSURE ON THE CAVITATION DAMAGE RATE OF 316 STAINLESS STEEL IN LIQUID POTASSIUM

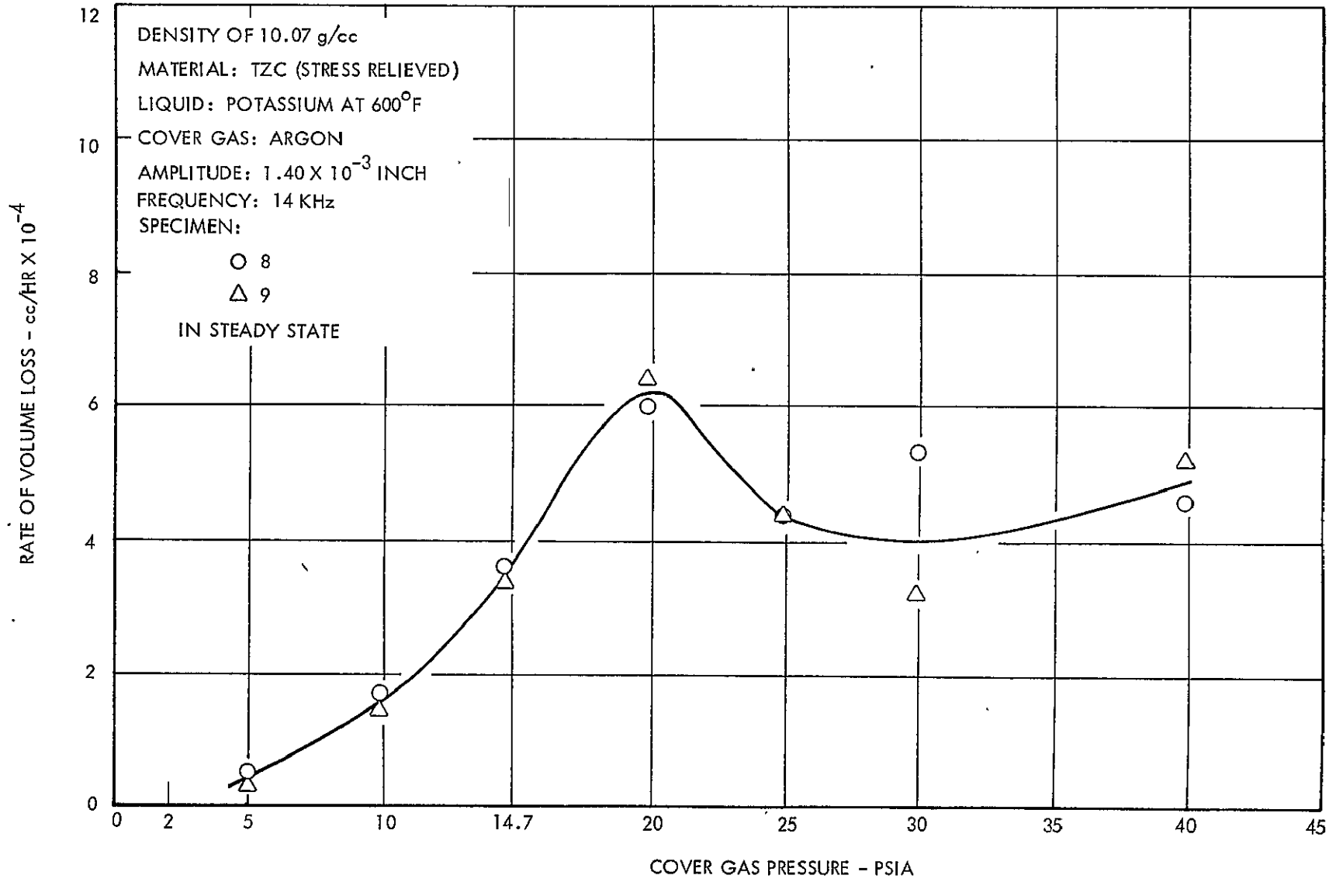

FIGURE 26 - THE EFFECT OF PRESSURE ON THE CAVITATION DAMAGE RATE OF TZC IN LIQUID POTASSIUM

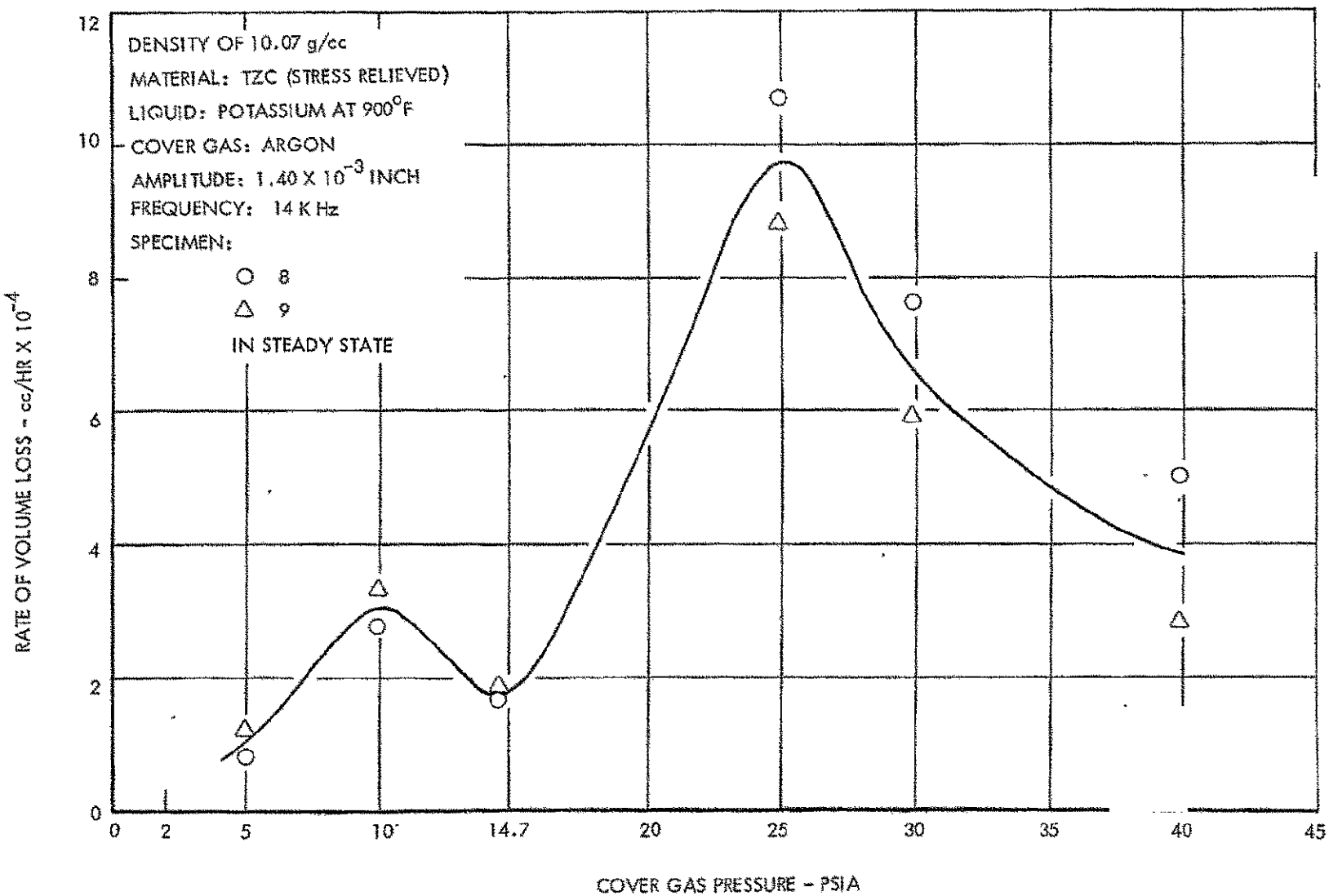

FIGURE 27 - THE EFFECT OF PRESSURE ON THE CAVITATION DAMAGE RATE OF TZC IN LIQUID POTASSIUM

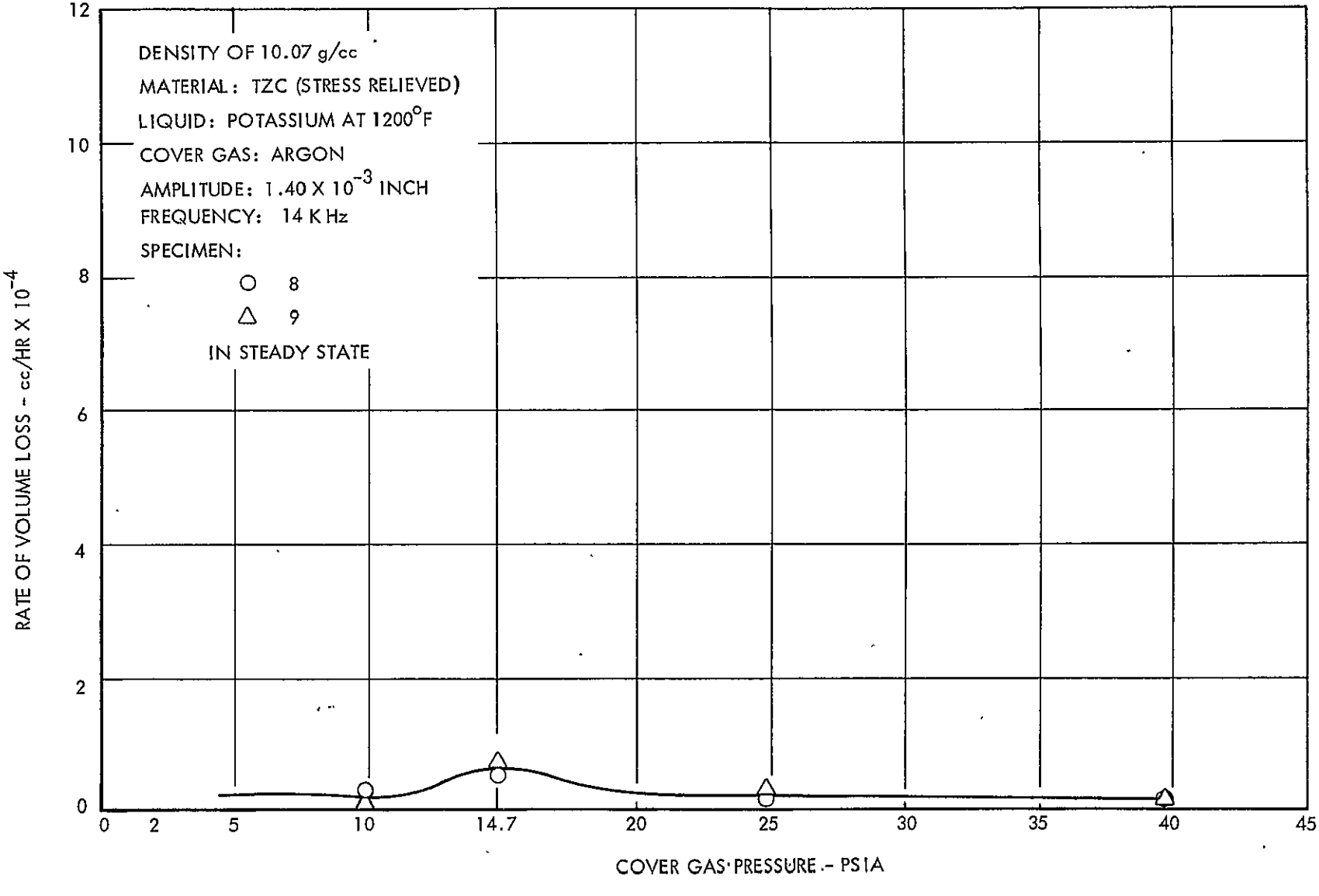

FIGURE 28 - THE EFFECT OF PRESSURE ON THE CAVITATION DAMAGE RATE OF TZC IN LIQUID POTASSIUM

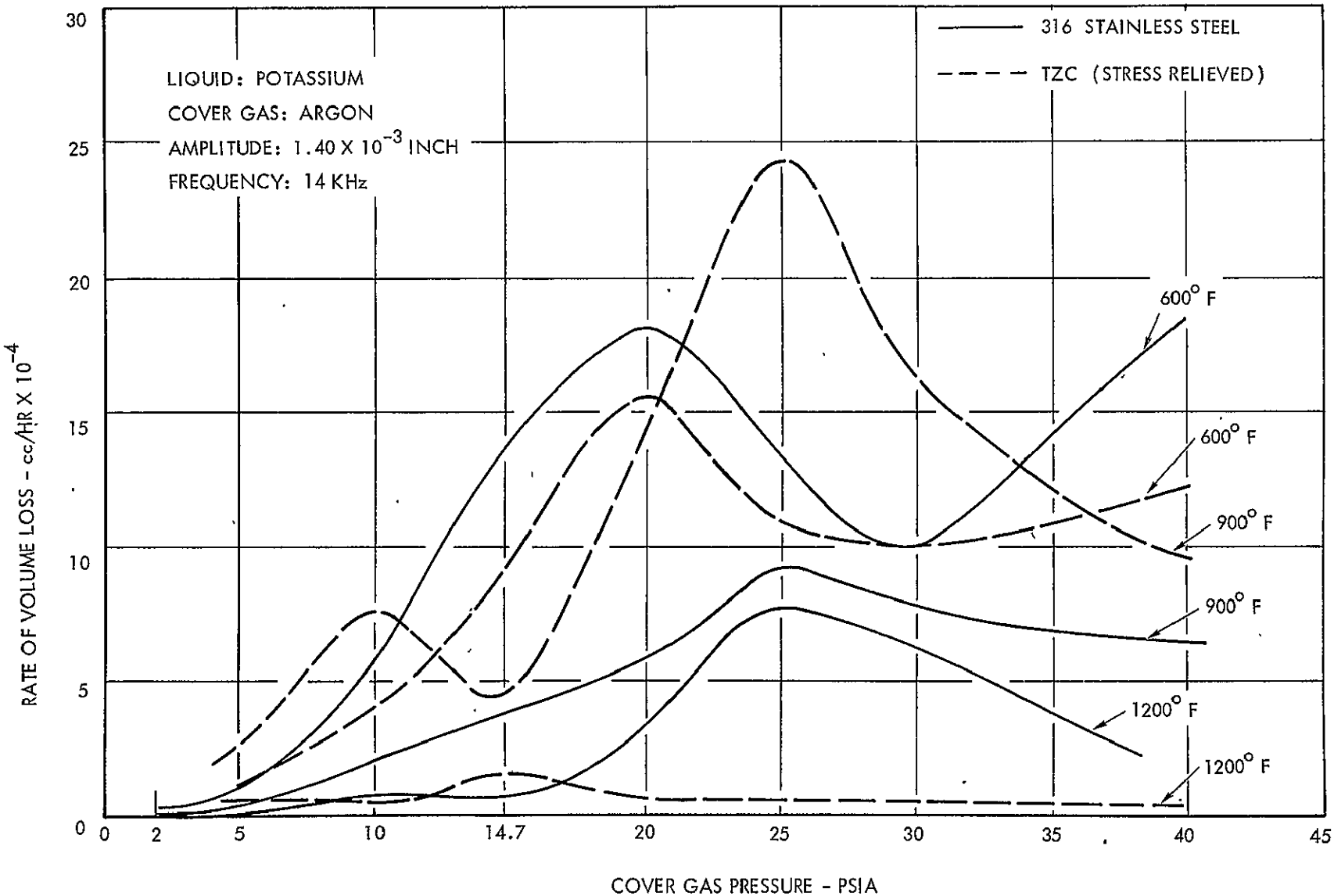

FIGURE 29 - COMPARISON OF THE EFFECT OF COVER GAS PRESSURE ON THE CAVITATION DAMAGE RATE OF REFRACTORY ALLOYS IN LIQUID POTASSIUM

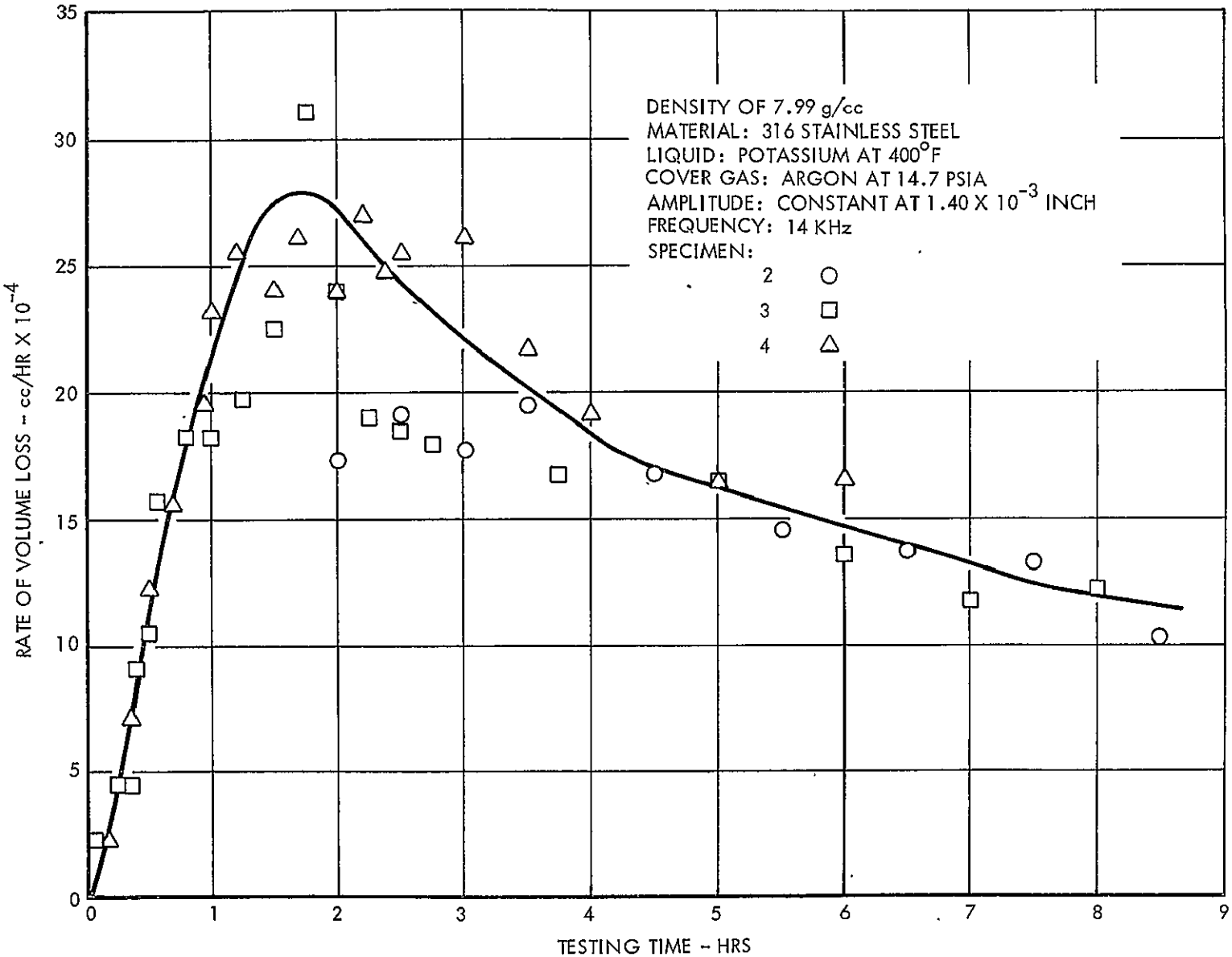

FIGURE 30 - EFFECT OF TESTING TIME ON CAVITATION DAMAGE RATE OF 316 STAINLESS STEEL IN LIQUID POTASSIUM

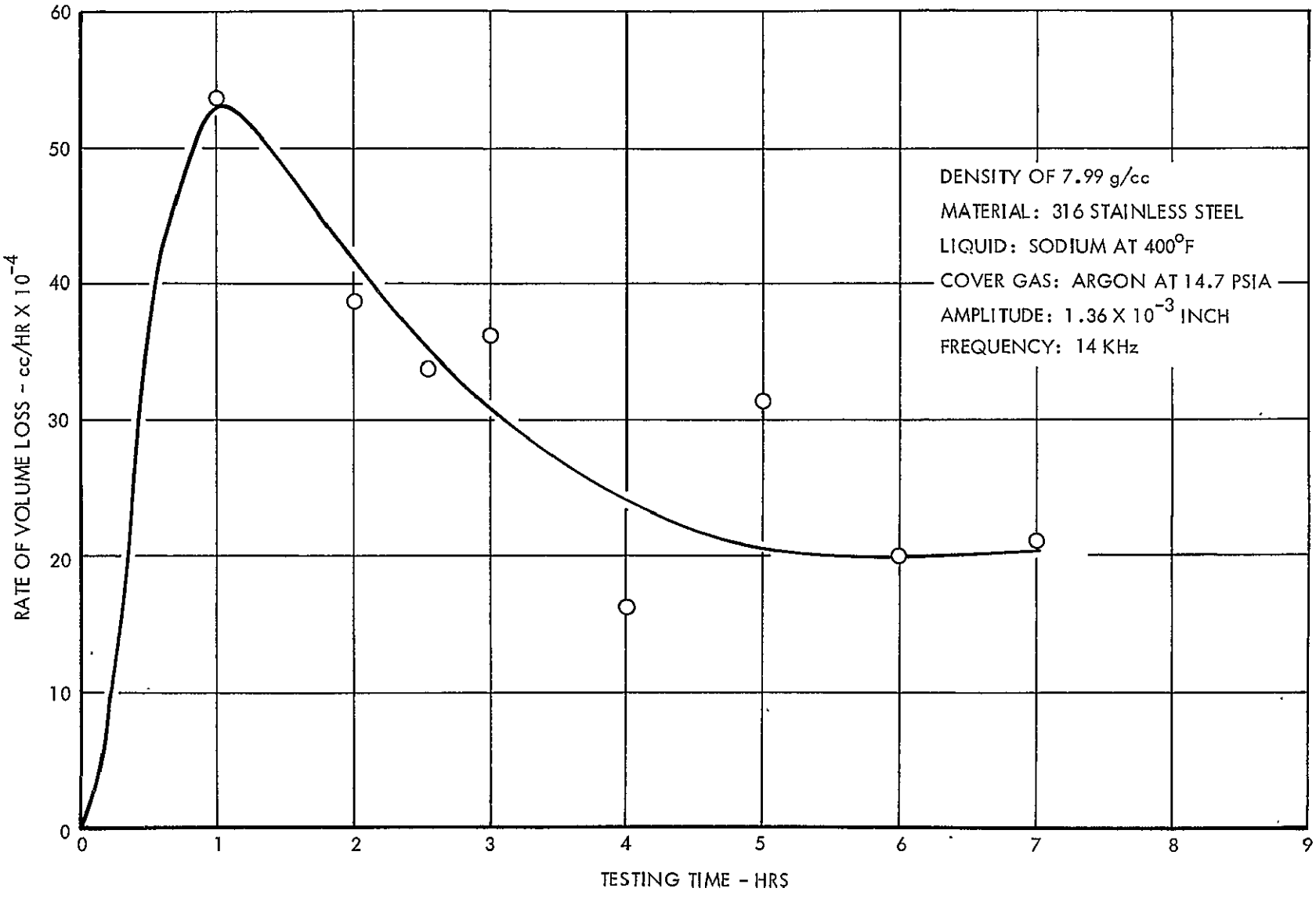

FIGURE 31 - EFFECT OF TESTING TIME ON CAVITATION DAMAGE RATE OF 316 STAINLESS STEEL IN LIQUID SODIUM

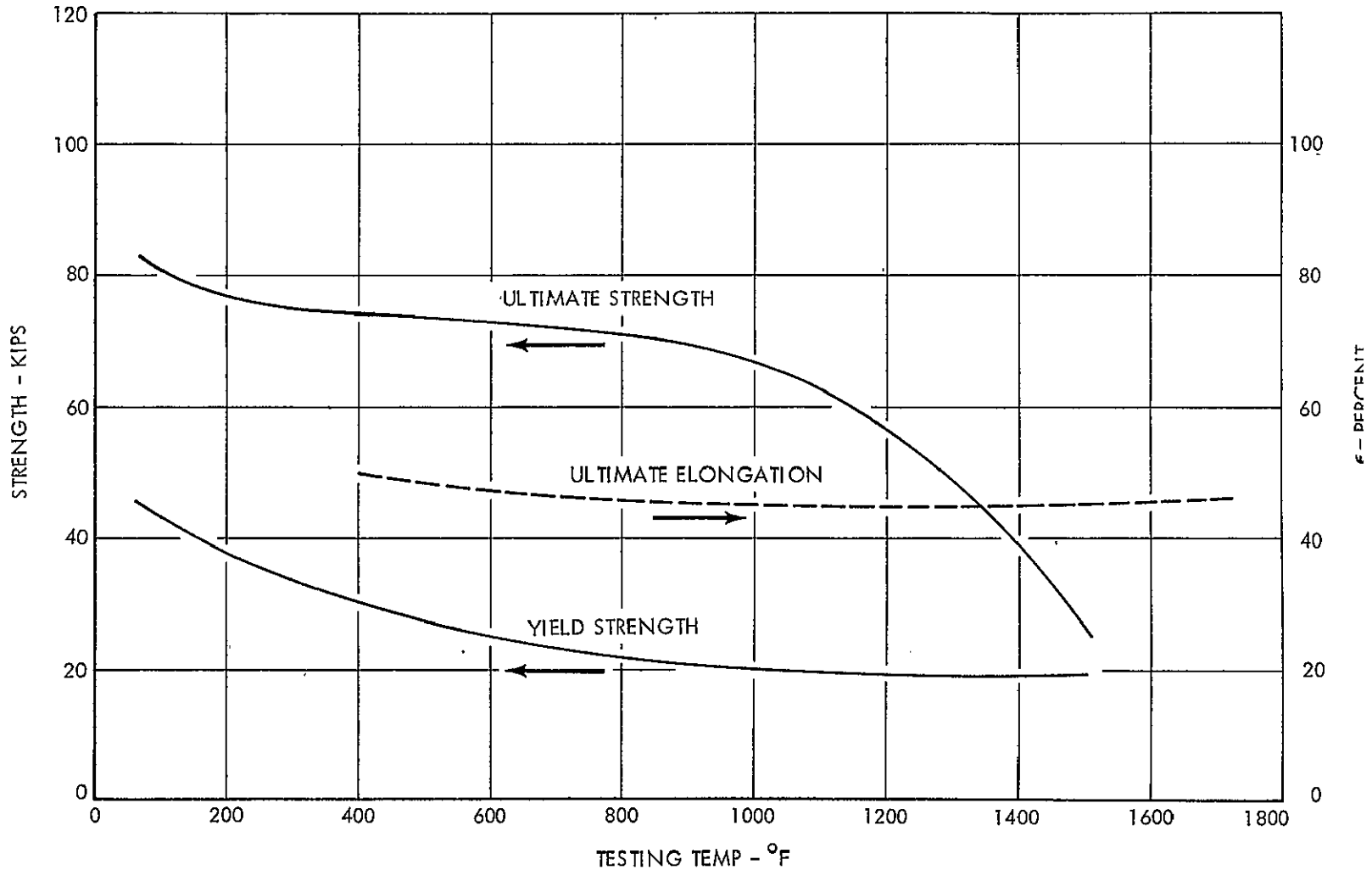

FIGURE 32- AVAILABLE MECHANICAL PROPERTIES OF 316 STAINLESS STEEL AT ELEVATED TEMPERATURES (DATA FROM REFERENCE 14)

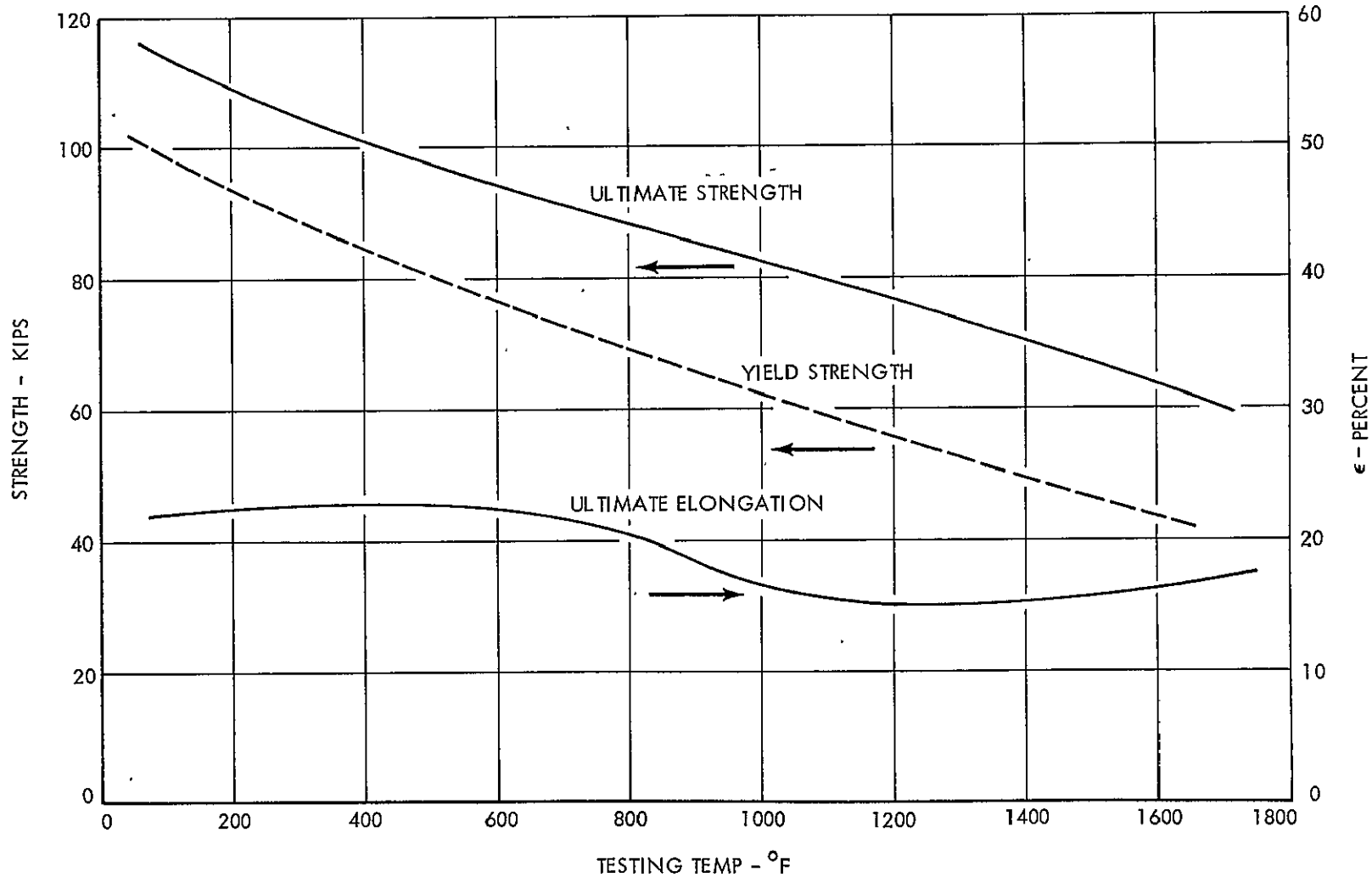

FIGURE 33- AVAILABLE MECHANICAL PROPERTIES OF TZC AT ELEVATED TEMPERATURES (DATA FROM REFERENCE 17)

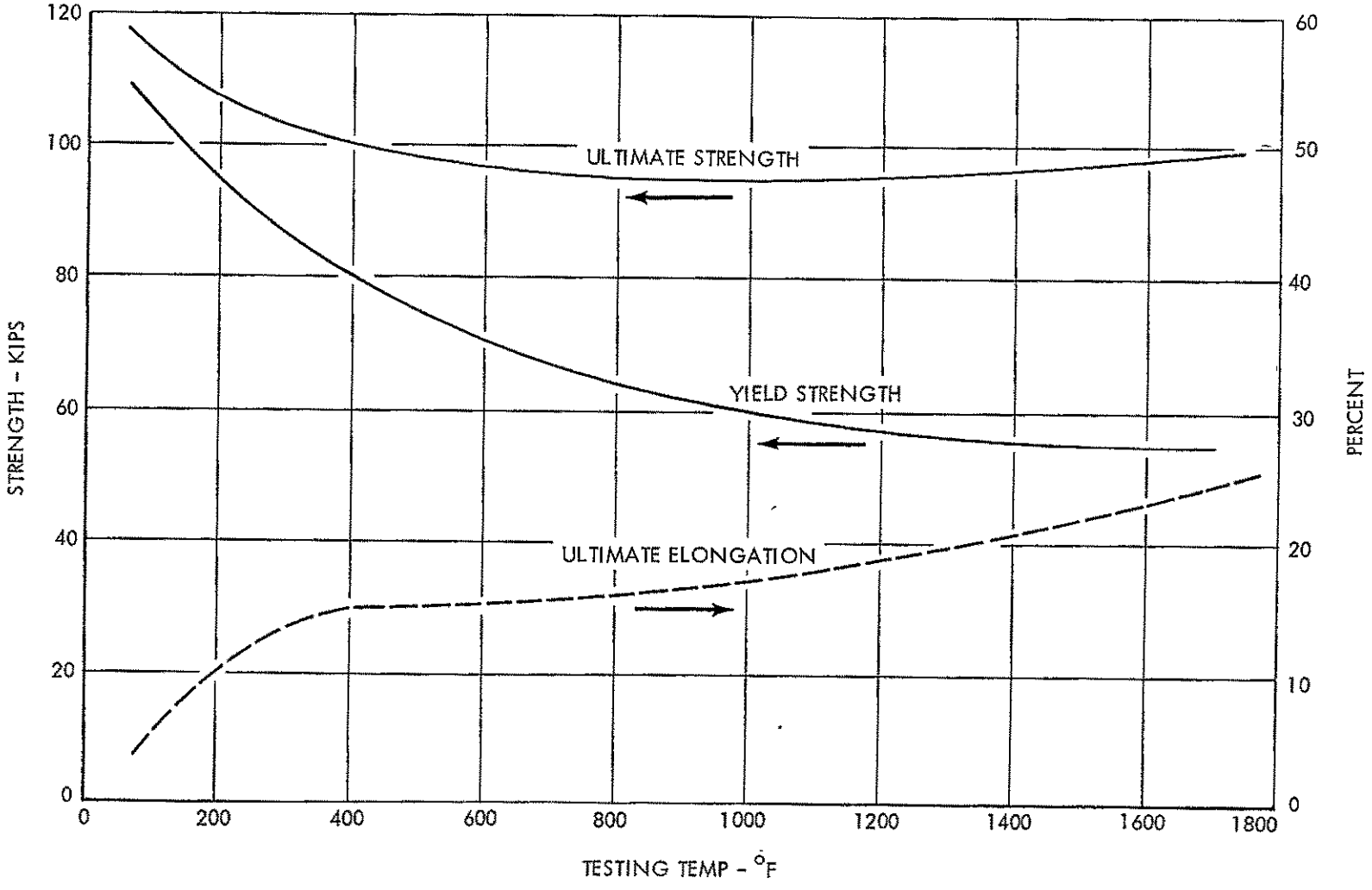

FIGURE 34 - AVAILABLE MECHANICAL PROPERTIES OF Cb-132M AT ELEVATED TEMPERATURES
(DATA FROM REFERENCE 15)

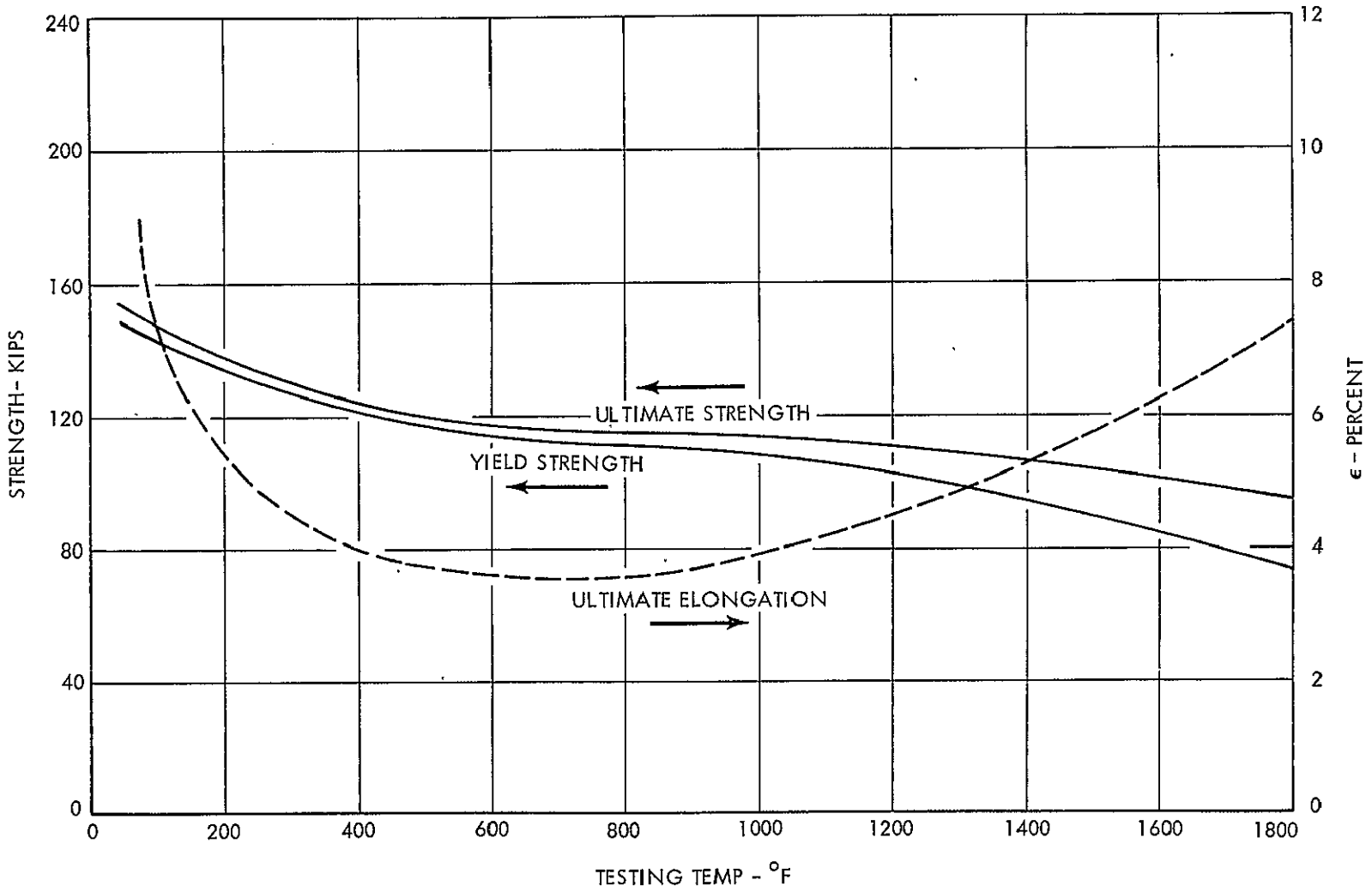

FIGURE 35 - AVAILABLE MECHANICAL PROPERTIES OF T-111 AT ELEVATED TEMPERATURES
(DATA FROM REFERENCES 16 AND 18)

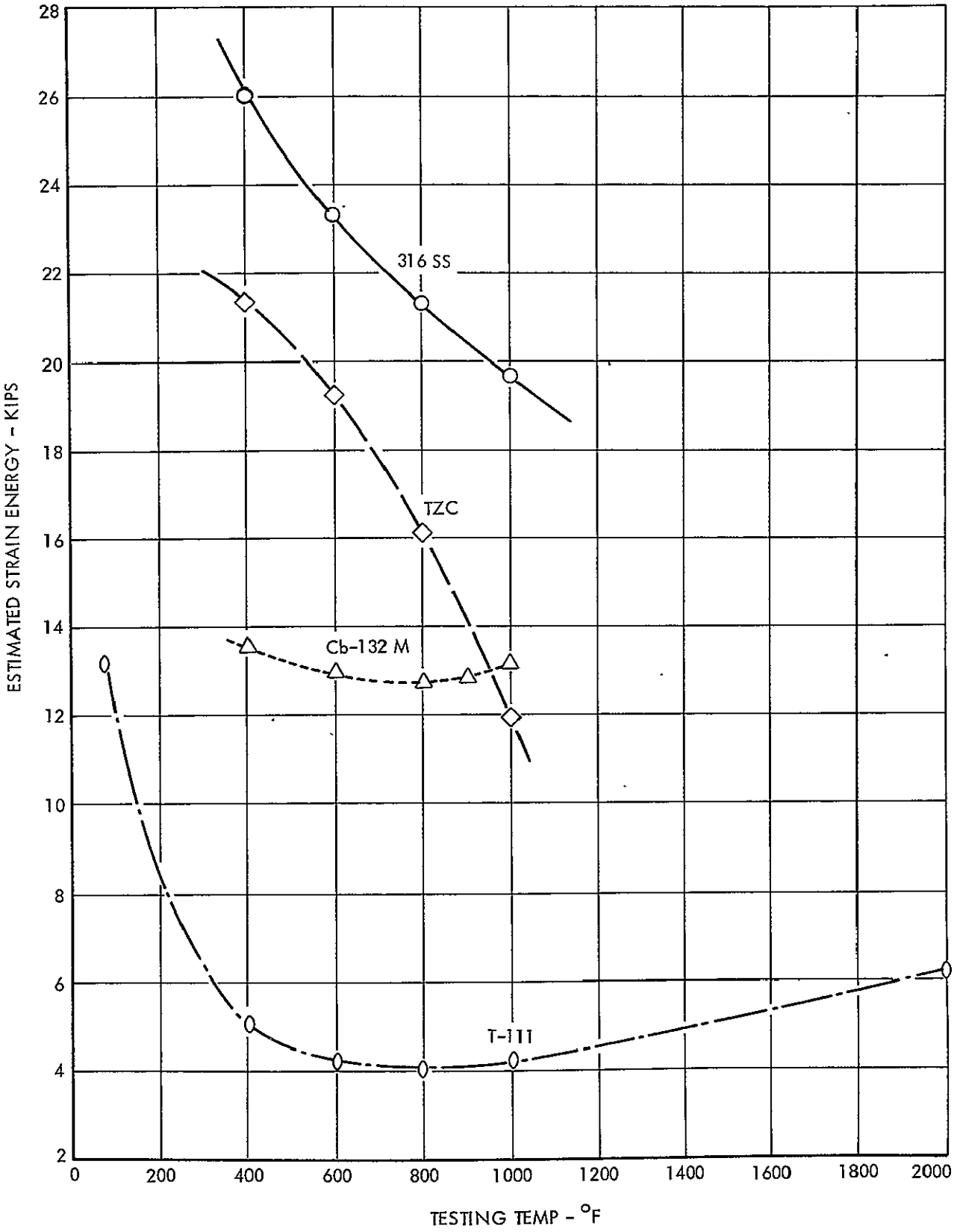

FIGURE 36 - EFFECT OF TEMPERATURE ON THE ESTIMATED STRAIN ENERGY OF FOUR REFRACTORY ALLOYS

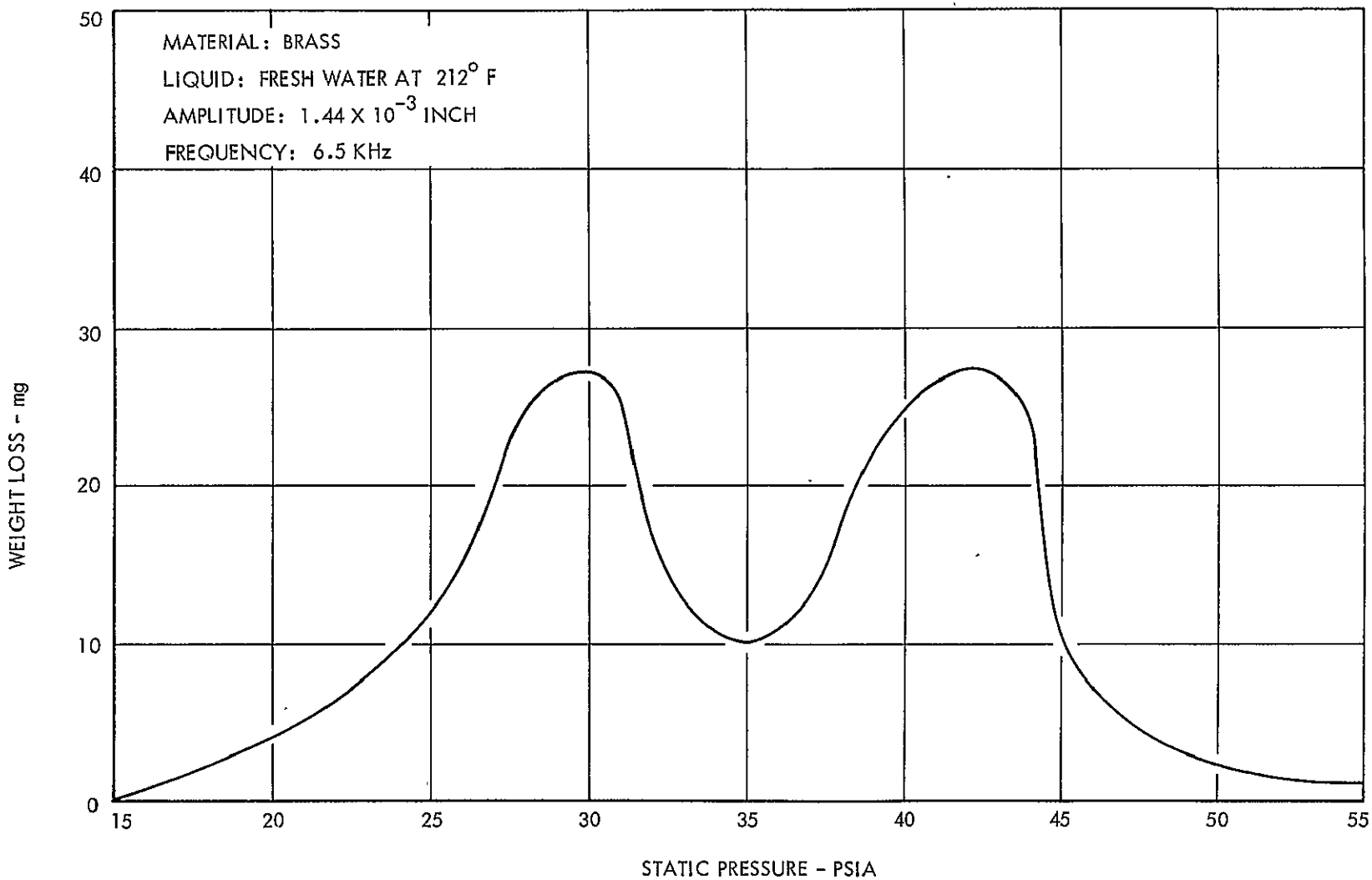

FIGURE 37 - EFFECT OF PRESSURE ON THE CAVITATION DAMAGE RATE OF BRASS (PETERS AND RIGHTMIRE)

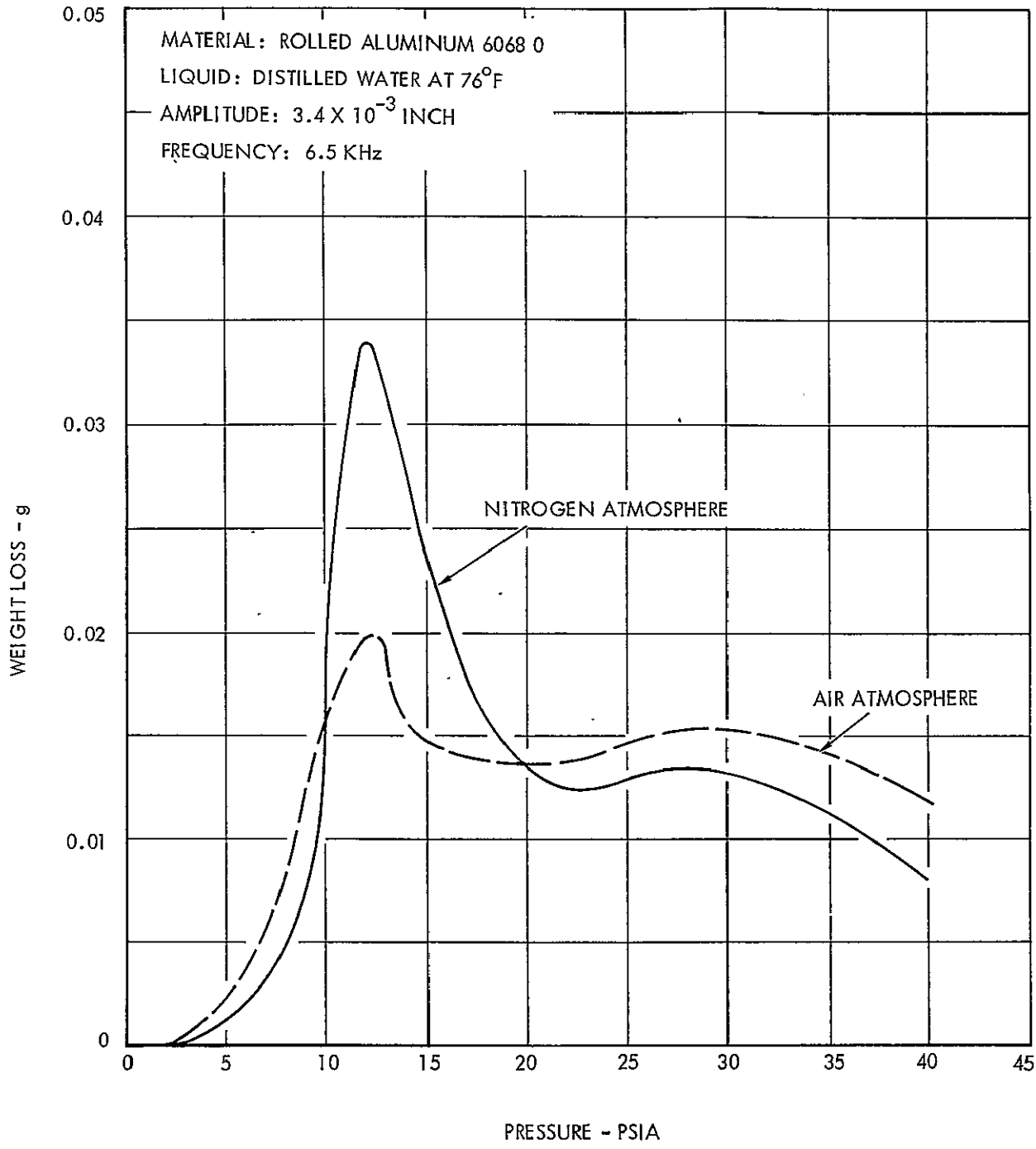

FIGURE 38 - EFFECT OF PRESSURE (LEITH AND THOMPSON)

Air Force Systems Command
Aeronautical Systems Div.
Wright-Patterson AFB, Ohio 45438
Attn: K. A. Davis (MANL) 1

Defense Documentation Center
Cameron Station
5010 Duke Street
Alexandria, Virginia 22314 2

Aerojet-General Corporation
SNAP-8 Division
Azusa, California 91703
Attn: Dr. Robert Gordon 1

General Electric Company
Missile and Space Division
Space Power and Propulsion Sect.
Cincinnati, Ohio 45215
Attn: Dr. J. W. Semmel 1
Dr. Olive Engle 1

University of Michigan
Nuclear Engr. Department
Ann Arbor, Michigan 48103
Attn: Dr. F. G. Hammitt 1

California Institute of Tech.
Dept. of Applied Mechanics
Pasadena, California 91103
Attn: Dr. M. S. Plesset 1

Westinghouse Electric Corporation
Astronuclear Laboratory
Box 10864
Pittsburgh, Penn. 15236
Attn: R. T. Begley 1

Atomics International
Liquid Metals Inf. Center
P. O. Box 309
Canoga Park, Calif. 91304
Attn: R.W. Dickinson 1

Defense Metals Inf. Center
Battelle Memorial Institute
505 King Avenue
Columbus, Ohio 43201 1

Allis-Chalmers Mfg. Company
York, Pennsylvania
Attn: W. J. Rheingans 1

TRW Inc.
Electromechanical Division
23555 Euclid Avenue
Cleveland, Ohio 44117
Attn: J. N. McCarthy 1

Philco Corporation
Aeronutronic Division
Ford Road
Newport Beach, Calif. 92660
Attn: H. D. Lindhardt 1

United Aircraft Corporation
Pratt and Whitney Aircraft Div.
400 Main Street
East Hartford, Conn. 06108
Attn: Dr. W.J. Lueckel 1

National Aeronautics and Space Administration
Jet Propulsion Laboratory
4800 Oak Grove Drive
Pasadena, Calif. 91103
Attn: Dr. Lance Hayes 1

HYDRONAUTICS, Incorporated

DISTRIBUTION LIST
(Contract No. NAS 3-8506)

National Aeronautics and Space Administration
Washington, D. C. 20546
Attn: J. J. Lynch, Code RNP 1
S.V. Manson, Code RNP 1

National Aeronautics and Space Administration
Ames Research Center
Moffett Field, Calif. 94035
Attn: Library 1

National Aeronautics and Space Administration
Langley Research Center
Langley Station
Hampton, Virginia 23365
Attn: Library 1

National Aeronautics and Space Administration
Lewis Research Center
21000 Brookpark Road
Cleveland, Ohio 44135
Attn: Dr. B. Lubarsky
MS 500-201 1
R. L. Cummings,
MS 500-201 1
J. P. Couch,
MS 500-201 2
M. J. Hartmann, MS 5-9 1
C.H. Hauser, MS 5-9 1
S.G. Young, MS 49-1 1
Library, MS 60-3 1
J.E. Dilley, MS 500-309 1
Tech. Utilization
Office, MS 3-19 1
Reliability and Quality
Assurance Office,
MS 500-203 1
Rpts Control, MS 5-5 1

National Aeronautics and Space Administration
Marshall Space Flight Center
Huntsville, Alabama 35812
Attn: Library 1

National Aeronautics and Space Administration
Scientific and Technical Information Facility
Box 5700, Bethesda, Md. 20014
Attn: NASA Representative 2

Jet Propulsion Laboratory
4800 Oak Grove Drive
Pasadena, Calif. 91103
Attn: Library 1

Argonne National Laboratory
P. O. Box 299
Lemont, Illinois 60439
Attn: Library 1

Brookhaven National Laboratory
Upton, New York 11973
Attn: Dr. O.E. Dwyer 1
Library 1

U. S. Atomic Energy Commission
Div. of Tech. Inf., Extension
P. O. Box 62
Oak Ridge, Tenn. 37831 2

Lawrence Radiation Laboratory
Livermore, California 94550
Attn: Dr. James Hadley
Head, Reactor Div. 1

North American Aviation, Inc.
Rocketdyne Division
6633 Canoga Avenue
Canoga Park, Calif. 91303
Attn: Robert Spies 1

Westinghouse Electric Corporation
Astronuclear Laboratory
P. O. Box 10864
Pittsburgh, Penn. 15236
Attn: W. D. Pouchot 1